INTERACTIONS OF ERISTOSTATIN WITH MELANOMA CELLS AND ITS EFFECTS ON NATURAL KILLER CELL CYTOTOXICITY

by

Alaa Mahmoud

A thesis submitted to the Faculty of the University of Delaware in partial fulfillment of the requirements for the degree of Honors Bachelor of Science in Medical Technology with Distinction.

Spring 2010

INTERACTIONS OF ERISTOSTATIN WITH MELANOMA CELLS AND ITS EFFECTS ON NATURAL KILLER CELL CYTOTOXICITY

by

Alaa Mahmoud

Approved: _____
Mary Ann McLane, Ph.D.
Professor in charge of thesis on behalf of the Advisory Committee

Approved: _____
Michelle A. Parent, Ph.D.
Committee member from the Department of Medical Technology

Approved: _____
Dallas G Hoover, Ph.D.
Committee member from the Board of Senior Thesis Readers

Approved: _____
Alan Fox, Ph.D.
Director, University Honors Program

ACKNOWLEDGMENTS

Special gratitude is due to Dr. Mary Ann McLane, my research advisor, for nurturing my passion for research. Through good times and bad, through my false proclamations of instant success, and my unconventional hypothesis, she remained supportive. I wish to also thank Dr. Michelle Parent for taking time out of her busy schedule to talk flow cytometry. For sharing her tissue culture expertise, I wish to extend a warm thank you to the tissue culture queen, Mollie Kostielney. And for making those long incubation periods on the third floor of desolate Willard Hall bearable, I owe my gratitude to Liana Sherrod, Torsten Joerger, and Sohil Golwala. To all the people I chased down and convinced to donate blood for this study, thank you. Your Natural Killer cells did not let you down. And to my family, I am truly grateful. Thank you all for the support and encouragement. You all are key factors in my motivation to keep on going.

This project was funded by INBRE-Delaware grant 2P20RR016472-09 (McL) and through University of Delaware Undergraduate Research Supply and Expense Grants.

I wish to dedicate this thesis to my baba, Mahmoud A. Mahmoud, who has dedicated his life to his three little boys. Your gracious unyielding support has truly made this possible. Thank you.

TABLE OF CONTENTS

LIST OF TABLES

LIST OF FIGURES

ABSTRACT

The ability of Natural Killer (NK) cells to lyse cancerous cells has been well documented. Interestingly, it has previously been shown that 4μM eristostatin, a snake venom disintegrin from *Eristocophis macmahoni*, elicits a 2-fold increase in the lytic ability of TALL-104 cells, NK-like cells, towards SbCl2, a radial growth phase melanoma cell line (McLane et al., 2001). Since TALL-104 cells exhibited a 2-fold increase in lytic ability towards SbCl2, it was hypothesized that eristostatin could also enhance the lytic ability of NK cells toward other melanoma cell lines (MV3, M24met, SbCl2, C8161, WM164, and 1205Lu). The lytic ability of NK cells was enhanced at select effector: target (E:T) ratios for several cell lines after a three hour incubation. However, with C8161, it was found that eristostatin suppressed the lytic ability of NK cells. The complexity of the study did not permit a general all encompassing answer to the question of whether eristostatin enhances the lytic ability of NK cells toward melanoma cells in general.

Although the aim of the study was to investigate the above mentioned question, it was found that eristostatin increased the survivability of certain melanoma cells *in vitro* after a three hour incubation; a finding worthy of further study.

Cytokine (Interferon-gamma (IFN-γ) and Tumor Necrosis Factor-alpha (TNF-α) studies were also conducted to further investigate the interaction of eristostatin with NK and melanoma cells. The effect of eristostatin on NK cell secretion of IFN-γ and TNF-α in the presence of four different melanoma cell lines was examined: 1205LU, M24met, MV3 (metastatic) SbCl2 (radial growth phase). It was notably found that when NK cells were incubated with 1205LU, there was a significant increase in the secretion of IFN-γ in the presence of 3μM eristostatin.

In addition, three-dimensional (3D) studies were performed to study the interactions of eristostatin with melanoma cells in a model that more closely resembles an *in vivo* model. The 3D studies were carried out in Matrigel®, a basement membrane harvested from Engelbreth-Holm-Swarm (EHS) mouse sarcoma. Matrigel® is comprised primarily of laminin, followed by collagen IV, heparin sulfate proteoglycans, and entactin/nidogen. Matrigel® also contains growth factors. To begin the three-dimensional studies, live/dead assays were performed in Matrigel® to see if cells incubated with eristostatin in a 3D environment exhibited similar live/dead ratios compared to cells incubated without eristostatin. It was found that cells in Matrigel® with or without eristostatin did not exhibit differences in spatial configuration or in live/dead ratios. It should be noted that eristostatin does not have inhibitory activity against cell adhesion to laminin or collagen. Since eristostatin inhibited melanoma cell migration on fibronectin (FN), future experiments will incorporate FN into the matrix (McLane et al., 2008).

Chapter 1

INTRODUCTION

1.1 Integrins

Integrins are transmembrane heterodimeric adhesion receptors composed of α and β subunits (van der Flier & Sonnenberg, 2001). Different combinations of eighteen possible alpha and eight possible beta chains linked in a non-covalent manner determine integrin-ligand specificity. Post-translational modifications also add to integrin diversity. There are 24 integrins that encompass the integrin family in humans (Humphries et al., 2004).

In spite of the diversity that exists among integrins, they primarily serve as adhesion molecules between cells and their surrounding extra-cellular matrix (ECM) (van der Flier & Sonnenberg, 2001). The ECM is a complex of high molecular weight proteins and polysaccharides made by cells that helps provide a matrix for growth factors and structural support, among other functions. Integrins with certain subunits adhere to certain components of the ECM. For example, integrins with α_4, α_5, α_8, α_{IIb}, or α_v bind to components of the ECM that contain the RGD structure found in fibronectin and vitronectin (van der Flier & Sonnenberg, 2001). In addition to mediating cell-ECM interactions, integrins can interact with counter-receptors found on other cells.

Integrins work by first adhering to their respective ligand then initiating an integrin cluster. Since integrin binding is usually weak, multiple integrins in a cluster binding to their ligand helps cells to adhere. Soon after, different cytoskeletal and

cytoplasmic proteins help anchor the complex to an actin cytoskeleton, in effect remodeling the actin cytoskeleton (van der Flier & Sonnenberg, 2001). The resulting complex is often referred to as a focal adhesion point, which plays an important role in signaling. It is also important to note that the I domain found on the extracellular domains of some α-subunits entails a characteristic metal ion-dependent (Mg^{2+}) adhesion site motif (MIDAS) (van der Flier & Sonnenberg, 2001). Sites like these are also believed to exist on β-subunits. Therefore, the presence of certain cations is required for proper integrin function.

1.2 Melanoma

Human skin is composed of three layers; the epidermis, the dermis, and the subcutis, collectively serving to maintain body temperature, to retain fluid, and to keep pathogenic microorganisms out of the body. The epidermis is the outer most layer and is composed of basal cells including melanocytes. Melanocytes produce melanin, a brown pigment that protects the skin when exposed to ultraviolet light.

In cases of melanoma skin cancer, the melanocytes typically found in the epithelial cell layer become malignant. Melanoma is less common than basal cell and squamous cell carcinomas. However, there is currently an epidemic of malignant melanoma in the United States with an estimated 62,480 new cases in 2008 that led to 8420 deaths (Reintgen et al., 2010).

Human melanoma cell lines (C8161, WM164, MV3, M24met, 1205Lu, SbCl2) were utilized for this study. Although melanoma cells are all malignant melanocytes, it is important to note the phase at which they were isolated. There are two phases of melanoma; radial growth phase and vertical growth phase melanoma (Urso, 2004). Vertical growth phase melanoma can further be classified into vertical

growth phase melanoma without metastatic competence and vertical growth phase melanoma with metastatic competence (Clark, 1991). In the radial growth phase, melanoma cells tend to grow into the epidermal layer and possibly into dermis but lack the ability to metastasize. In vertical growth phase, melanoma invades the dermis and can be metastatically competent. SbCl2 is the only radial growth phase melanoma used in this study (Sturm et al., 2002). WM164 was isolated as a vertical growth phase melanoma that did not metastasize (Herlyn et al., 1990). The other cell lines (1205Lu, C8161, M24Met, MV3) were all vertical growth phase melanomas isolated from metastatic sites (Juhasz et al., 1993)(Bregman et al., 1986)(Mueller et al., 1991) (van Muijen et al., 1991).

It must be noted that in order for melanoma cells to metastasize, they must first migrate from the primary tumor site to a secondary site then adhere, a process that requires integrins.

1.3 Eristostatin

Disintegrins are a group of small (4-16kDa), naturally occurring, cysteine-rich proteins isolated from viper snake venoms of four families; *Atractaspididae, Elapidae, Viperidae, and Colubridae* (McLane et al., 2008). Disintegrins can exist as monomers or dimers and bind integrins in a dose-dependent manner. Monomeric disintegrins are classified according to size such that 41-51 residues and 4 disulfide bonds constitutes a short disintegrin, approximately 70 residues and six disulfide bonds constitutes a medium disintegrin, and roughly 84 residues and 7 disulfide bonds constitutes a long disintegrin. The binding mechanism of disintegrins involves primarily the "RGD adhesive loop," an R/K/M/W/VGD, MLD, MVD or K/RTS sequence (McLane et al., 2008).

Eristostatin is a monomeric short disintegrin isolated from the venom of *Eristicophis macmahoni* (McLane et al., 2005). It inhibits platelet aggregation and binds platelets independent of activation (McLane et al., 1994). Eristostatin also inhibits human as well as murine melanoma cell metastasis *in vivo* (McLane et al., 2001). In spite of the amount of research done on eristostatin, the mechanism of its interaction with melanoma cells remains unclear. Eristostatin, however, interacts with αIIbβ3 on platelets (McLane et al., 1994) and did demonstrate an interaction with α4β1 on MV3 melanoma cells (Danen et al., 1998). Unlike a majority of other disintegrins, eristostatin does not interact with αvβ3 or α5β1 (Wierzbicka-Patynowski et al., 1999). Overall, eristostatin is a unique disintegrin and remains an area worthy of further research.

1.4 Natural Killer (NK) Cells

NK cells are lymphocytes of the innate immune system that possess cytotoxicity against tumor cells along with antiviral properties (Moretta & Moretta, 2004). NK cells have a series of receptors on their surface; some of which are activating and some of which are inhibitory. The sum of these interactions determines whether an NK cell can be activated (Vivier et al., 2008). A main inhibitory receptor used by NK cells is the Major Histocompatibility (MHC) class 1 receptor. MHC I, essential in discriminating between self and non-self, is used by NK cells to differentiate between healthy cells and cells in distress (Anfossi et al., 2006). It is important to note that resting human NK cells in the peripheral blood exhibit poor effector capabilities and must be 'primed' prior to use *in vitro* assays (Vivier et al., 2008).

There are two subsets of NK cells in humans; $CD56^{bright}$ and $CD56^{dim}$ grouped depending on the density of CD56 on their surface (Cooper et al., 2001). Composing nearly 90% of NK cells in the peripheral blood, $CD56^{dim}$ NK cells are innately more cytotoxic while $CD56^{bright}$ NK cells produce more abundant cytokines (Cooper et al., 2001). However, $CD56^{dim}$ do produce IFN-γ when they interact with tumor cells *in vitro* (Vivier et al., 2008).

1.5 IFN-γ and TNF-α

During both the innate and specific immune responses, macrophage are stimulated by various cytokines including Interferon gamma (IFN-γ). IFN-γ is part of a group of a group of cytokines referred to as IFNs. IFNs are divided into two types based on sequence homology and receptor specificity (Schroder et al., 2004). Originally referred to as macrophage activating factor, IFN-γ is the only member of the type II IFNs (Schroder et al., 2004).

IFN-γ has various effects on macrophages including the up-regulation of antigen processing and presentation pathways and direct anti-tumor and anti-bacterial mechanisms (Schroder et al., 2004). In addition to its effects on macrophages, IFN-γ also plays other important roles including attracting leukocytes to a localized site and impacting the growth and differentiation of various cell lines. IFN-γ also regulates B cell function and enhances the activity of NK cells (Schroder et al., 2004).

IFN-γ is produced by Type 1 T helper cells (CD 4+), cytotoxic T cells (CD8+), and Natural Killer cells. However, new evidence suggests that this list is not all inclusive and that B cells, NKT (heterogeneous population of cells that shares NK and T cell properties), and antigen-presenting cells also secrete IFN-γ. For the most part, secretion of IFN-γ is up-regulated by specific cytokines, most notably interleukin

(IL)-18 and IL-12 and is down regulated by IL-4, IL-10 among others. These cytokines are often products secreted by antigen-presenting cells.

Although first described in 1975, all of the functions of the inflammatory cytokine, TNF-α, remain unclear (Helson et al., 1975). Secreted by different cells, notably by macrophages after stimulation with bacterial lipopolysaccharide (LPS), TNF-α acts as a regulator of immune cells (Vassalli, 1992). However, its regulation mechanisms are often complex. For instance, TNF-α inhibits the apoptosis of neutrophils at 20 hours, but interestingly stimulates apoptosis in a subpopulation of neutrophils at 2-8 hours (Murray et al., 1997). TNF-α also serves as an activator of monocytes and macrophages and also induces their differentiation (Vassalli, 1992). Similarly, TNF-α also enhances B cell growth and maturation (Vassalli, 1992). In the presence of IL-2, TNF-α serves to increase the number of IL-2 receptors on NK cells while increasing their lytic ability (Vassalli, 1992).

In addition to acting as a regulator of immune cells, TNF-α also has a notable cytotoxic property against a variety of human and mouse tumors and has antiviral properties (Vassalli, 1992). Systemically in low doses, TNF-α can induce fever and a generalized inflammatory condition while high doses result in septic shock-like symptoms (Vassalli, 1992). Overall, TNF-α induces a series of complex reactions important in many immune reactions *in vivo*, including malignancies.

Chapter 2

METHODS

2.1 Isolation of NK Cells

Whole blood (~50mL) was collected aseptically by venipuncture into 150 USP units of spray-coated sodium heparin vacutaner tubes. Tubes of blood were inverted several times to ensure inhibition of coagulation. The tubes of blood, phosphate buffered saline (PBS) with 2% (v/v) fetal bovine serum (FBS), Ficoll-paque, and RosetteSep Human NK enrichment cocktail from Stemcell Technologies (Vancouver, Canada) were allowed to equilibrate to room temperature prior to the isolation of NK cells.

Heparinized blood (20mL) was transferred into conical tubes and 1000uL of RosetteSep Human NK enrichment cocktail was added. This cocktail includes antibodies to Glycophorin A, CD3, CD4, CD19, CD36, and CD66b. Therefore, NK subsets with the markers above were not included. For instance, NKT cells with CD3 were not in the NK population used. However, these populations make up a minute percentage of the NK cells isolated. After adding the RosetteSep, the conical tubes were inverted gently and allowed to incubate at room temperature for 20 minutes.

Following incubation, an equal volume of PBS with 2% FBS was added to each conical tube. Tubes were inverted gently to mix. Ficoll-paque (15mL) was added to new conical tubes. The blood-cocktail-PBS mixture (20mL) was gently pipetted over the ficoll-paque to ensure that the blood stayed on top of the column and

did not mix into the ficoll-paque. The column was centrifuged at 1200g at room temperature for 20 minutes with the brake off.

The columns were removed from the centrifuge gently to prevent re-mixing. A 1000uL pipette was used to aspirate 8-10mL of NK cells from the Ficoll-paque-plasma interface (Figure 1). In certain cases, removing the plasma layer prior to removing the NK layer helped locate the NK region. However, using this strategy risked losing some NK cells.

Isolated NK cells were added to a new conical tube and overlaid with an equal volume of PBS with 2% FBS. The cells were centrifuged at 300g for 10 minutes at room temperature. After the supernatant was discarded, the cell pellet was resuspended in 5mL of RPMI (named after Roswell Park Memorial Institute where it was made) with 10% FBS and transferred to a 100mm tissue culture plate. Some of the cell suspension (~200uL) was aliquoted for flow cytometry to assess purity by staining with FITC-labeled anti-CD56 from Invitrogen (Camarillo, CA) or with FITC-labeled IgG2a isotype control from Invitrogen (Camarillo, CA). IL-2 (750U/mL) was added to each dish, and cells were incubated at 37°C with 5% CO_2. NK cells were usually used for assay after an overnight incubation. However, if cells were not used the following day, they were supplemented with more IL-2 (750U/mL).

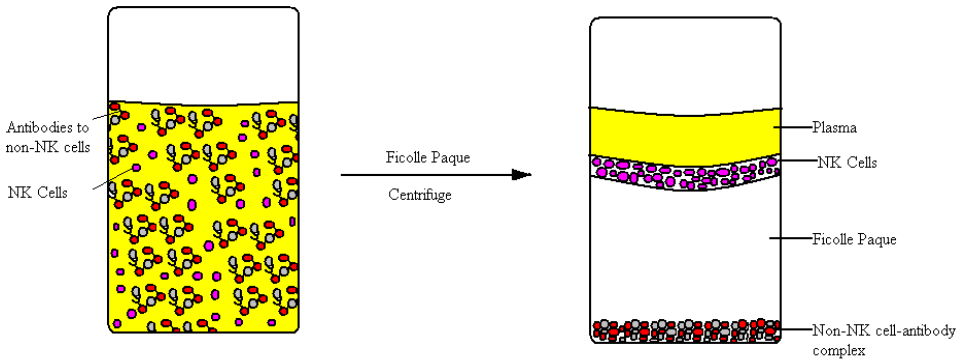

Figure 1 Isolation of Natural Killer Cells via RosetteSep.

2.2 Cell Culture

Melanoma cell lines (1205Lu, M24met, MV3, SbCl2, C8161, WM164) were thawed and kept in Dulbecco's Modified Eagle Medium with 10% FBS (DMEM-F12) at 37ºC with 5% CO_2. Prior to assays, the media was aspirated and 1mM EDTA was added. The cells were incubated at 37ºC with 5% CO_2. Following incubation, the cells were resuspended in PBS and centrifuged at 700g for five minutes at 4°C. The PBS was aspirated off the cell pellet and the cells were resuspended in fresh PBS. A 10uL sample of the suspension was treated with 90uL of Trypan Blue and counted on a hemacytometer. Four primary squares were counted and final stock concentration was determined using the following formula:

$$\textbf{[number of cells counted]/4 x 10 = cells} \times 10^6/\textbf{ml}$$

Using the answer above, the suspension was diluted to get the desired cell concentration.

2.3 Three Dimensional (3D) Studies

Phenol red free Matrigel® (BD Biosciences, Bedford, MA) was thawed overnight in a container of ice placed at 4°C. Prior to setup, 8-well glass chamber slides and pipette tips were cooled on ice. Borosilicate sterile 8-well glass chamber slides (#1.5) were purchased from LAB-TEK (Naperville, IL). Matrigel® (40uL) was placed into each chamber and spread to cover the bottom without forming air bubbles. The 8-well glass chamber slides were incubated at 37°C with 5% CO_2 for a minimum of 15 minutes to solidify the 100% Matrigel® base. Melanoma cells were concentrated to 2.5 x 10^4 cells/mL in DMEM-F12 with 10% FBS (see cell culture) and kept on ice until the following step. In a separate conical tube, a 4% Matrigel®, 6μM eristostatin suspension was prepared in DMEM-F12 with 10% FBS and the solution was kept on ice to prevent the Matrigel® from solidifying. Equal volumes of the cell suspension and the Matrigel®-eristostatin-DMEM-F12 with 10% FBS solution were mixed by pipetting up and down and inverting gently. Final concentrations were 3μM eristostatin, 1.25 x 10^4 melanoma cells/mL, and 2% Matrigel®.

The chamber slides were removed from the incubator and 400uL of the prepared solution was added to all the wells. The slides were incubated at 37°C with 5% CO_2. On days one, three, and five of incubation, two 8-well glass chambered slides were removed from the incubator and stained with propidium iodide (1.46 μg/mL) (Molecular Probes, Eugene, OR) and Syto (12.5μM) (Molecular Probes, Eugene, OR). After staining, the wells were observed via confocal microscopy. The Zeiss LSM 510 VIS attached to an Axiovert 100M was used for imaging. The well was scanned under low power (100x) for overall distribution of the cells and structures were evaluated at 200x for spatial configuration and patterns in the well with eristostatin and those without.

2.4 Flow Cytometric Cytotoxicity Assay

A MitoTracker Green FM (Invitrogen Eugene, OR) vial was reconstituted with dimethyl sulfoxide (DMSO) according to directions on the vial label, creating a 1mM stock solution. The vial was vortexed and allowed to sit at room temperature for 5 minutes. The vial was vortexed again and reconstituted stock was diluted with PBS to make a 10^{-5} M working solution.

A 10^6 cells/mL suspension was prepared (refer to tissue culture section) of melanoma cells. MitroTracker Green FM was added to the cell suspension (final concentration 300nM) and the suspension was incubated in a water bath at 37°C for 20 minutes along with a no-stain control. The cells were washed with Phosphate Buffered Saline (PBS) three times (150G, 5 minutes, 4°C), resuspended in phenol red-free RPMI with 10% FBS. An aliquot of stained cells was treated with 3µM eristostatin, and another aliquot was treated with sterile distilled water.

For some experiments, the NK cell concentration obtained by the hemacytometer formula was inserted into a computer algorithm to determine the volumes of NK cell suspension needed to prepare the appropriate E:T ratios. The ratios of E:T cells were prepared in sterile v-bottom plates. The plates were spun at 30 seconds at room temperature at 200G and incubated for three hours at 37°C with 5% CO_2 and analyzed via flow cytometry (Figure 2). All error bar presented in the results section are standard error calculations.

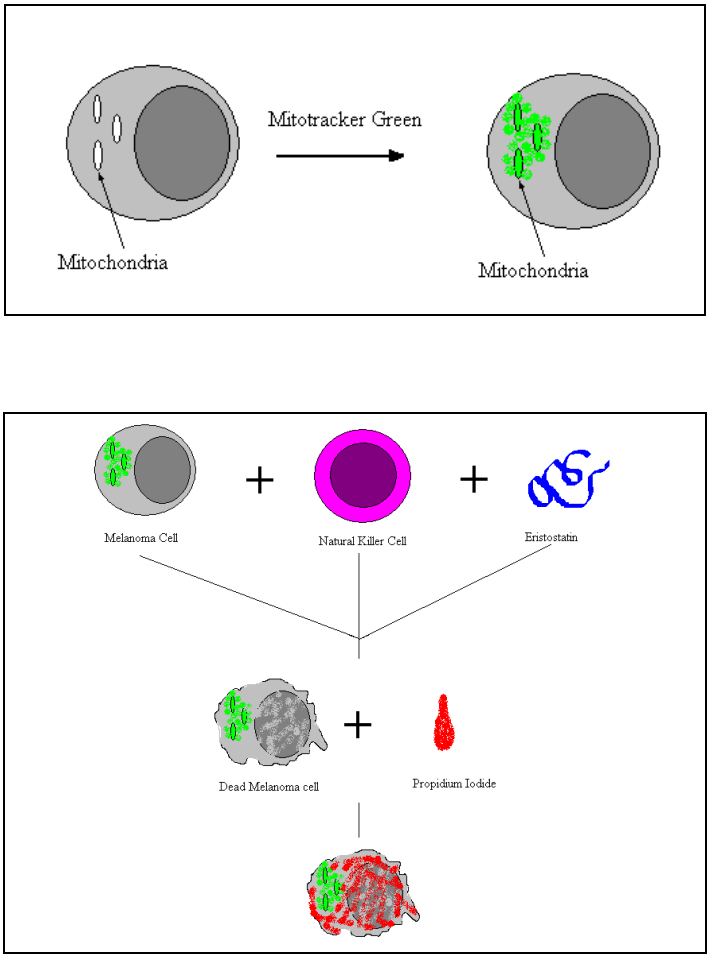

Figure 2 **Flow Cytometry Cytotoxicity Assay.** The mitochondria are stained with Mitotracker Green, and Propidium Iodide is used to detect dead cells via flow cytometry.

2.5 CytoTox-Glo Cytotoxicity Assay

A melanoma cell suspension (10^6 cells/mL) was prepared as described in section 1.2. In a 35mm plate, cells were treated with either 3µM eristostatin or sterile deionized water. NK cell concentration was adjusted to $1.1x10^6$ cell/mL as described in section 1.2. Ratios of T:E and control wells (just melanoma cells and just serum-free DMEM w/ F12) were transferred into a sterile 96-well luminescence compatible plate from Packard (Neriden, CT). The plates were incubated overnight at 37°C with 5% CO_2.

The following day, reagents (AAF-Glo Substratre, Assay Buffer, Digitonin) (Promega Corporation, Madision, WI) were thawed in a 37°C water bath. The contents of one assay buffer bottle were transferred into a substrate bottle according to manufacture recommendations. The lysis buffer was prepared by adding 13µL of digitonin to 2.75mL of assay buffer (94.5 µg/mL).

The 96-well plate was removed from the incubator and 50µL of CytoTox-Glo Reagent was added to all wells. The plate was placed on a orbital shaker (~200rpm) for 4 minutes and incubated at room temperature for 15 minutes. The luminescence was read on a Fusion plate reader (Perkin Elmer, Wellesley, MA).

After the reading, 50µL of lysis buffer was added to all wells. The plate was once again shaken at ~200rpm for 4 minutes and incubated at room temperature for 15 minutes. The final luminescence was determined using a Fusion plate reader (Perkin Elmer, Wellesley, MA). Luminescence due to NK and media was subtracted and the luminescence prior to lysis and after lysis was used to calculate percent lysis.

[Initial Luminescence - Initial NK Luminescence - Media Luminescence]/[Post Lysis Luminescence - Post Lysis NK Luminescence – Post Lysis Media Luminescence]*100 = Percent Lysis

2.6 Human IFN-γ

Supernatants were aspirated from varying E:T ratios incubated overnight with eristostatin at 37°C with 5% CO_2 and stored at -80°C until the experiment could be run. 96-well plates containing immobilized anti-IFN-γ and all assay reagents were acquired from Assay Designs (Ann Arbor, MI). Wash buffer was prepared according to manufacture recommendations (1450mL of deionized water and 50mL of wash buffer concentrate). Prior to assay, frozen supernatants were thawed using by gently rolling between palms. The reagents and standard were thawed at room temperature for ≥ 30 minutes before the assay. The standard was reconstituted according to manufacture recommendations with deionized water and was then serially diluted into 1.5mL polypropylene tubes using RPMI 10%FBS to construct the standard curve.

Biotinylated anti-IFN-γ (50µL) was added to each well except the blank wells. Samples, standards, and RPMI 10% FBS were added to their respective wells. The plate was sealed with a plate sealer and incubated at room temperature for 2 hours.

Streptavidin-Horseradish Peroxidase (HRP) solution (Assay Designs, Ann Arbor, MI) was prepared during the incubation. The contents of the plates were discarded by inversion, and each well was washed three times with wash solution. Freshly prepared Streptavidin-HRP conjugate was added to each well except the blank well. The plates were sealed and incubated at room temperature for 30 minutes.

The contents were emptied again, and each well was washed three times with wash solution. Substrate was added to each well and the plate was sealed and incubated in the dark for 30 minutes. Following incubation, stop solution was added to each well. The plate reader was blanked against the blank wells and readings were taken at 450nm with correction at 570 and 590nm. This assay is described as an

enzyme-linked immunosorbent assay (ELISA) and the mechanism is shown in Figure 3. Extrapolation from standard curve was used to determine the concentration of IFN-γ (Figure 4). All ratios were run in duplicate and averaged prior to graphing. In addition, a blank well with RPMI with 10% FBS was subtracted from all ratios.

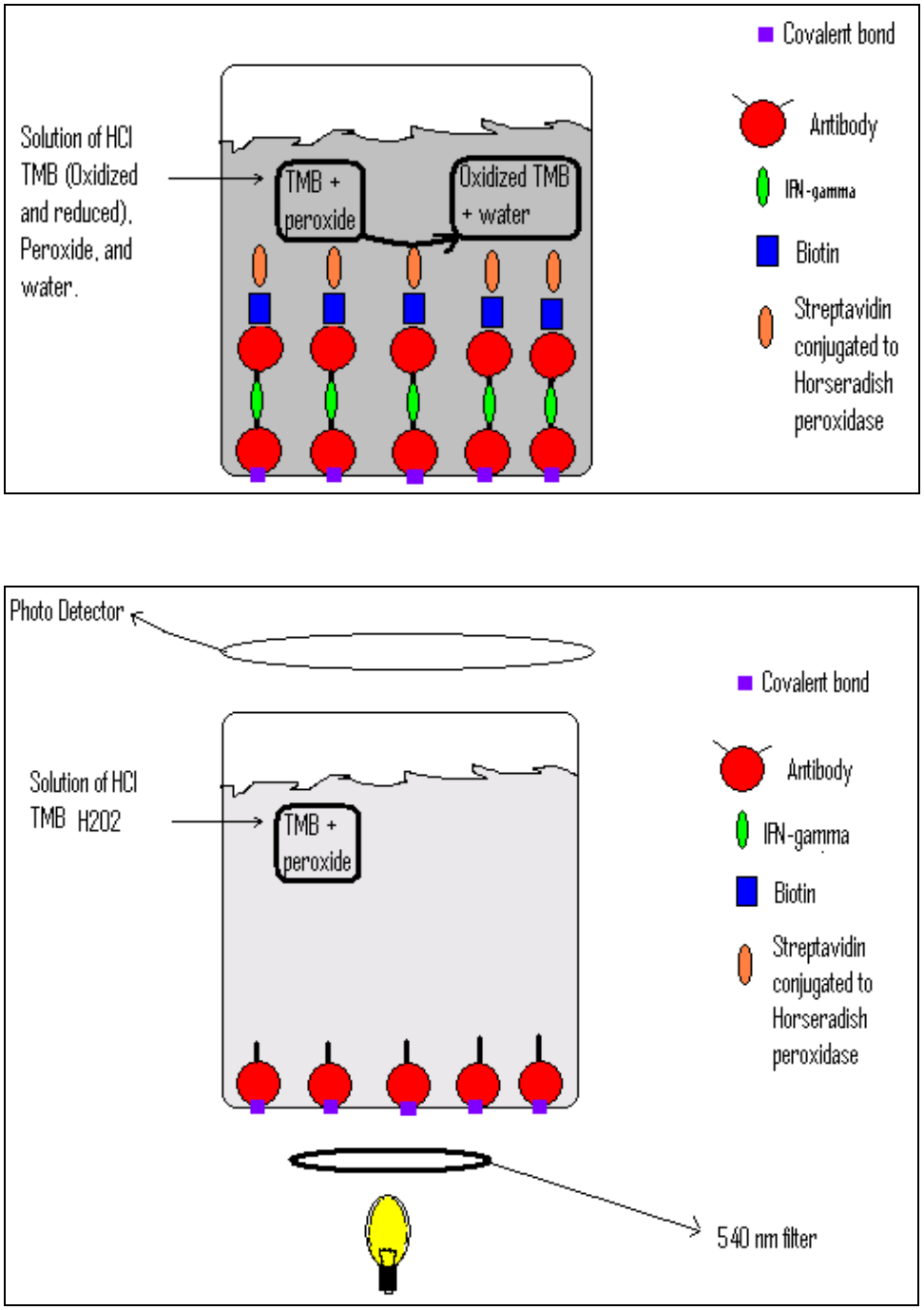

Figure 3 **Mechanism of Measuring Cytokines via ELISA.** Top: The more IFN-γ in the samples, the more streptavidin is available to oxidize TMB. Bottom: If no IFN-γ is present, not TMB is oxidized.

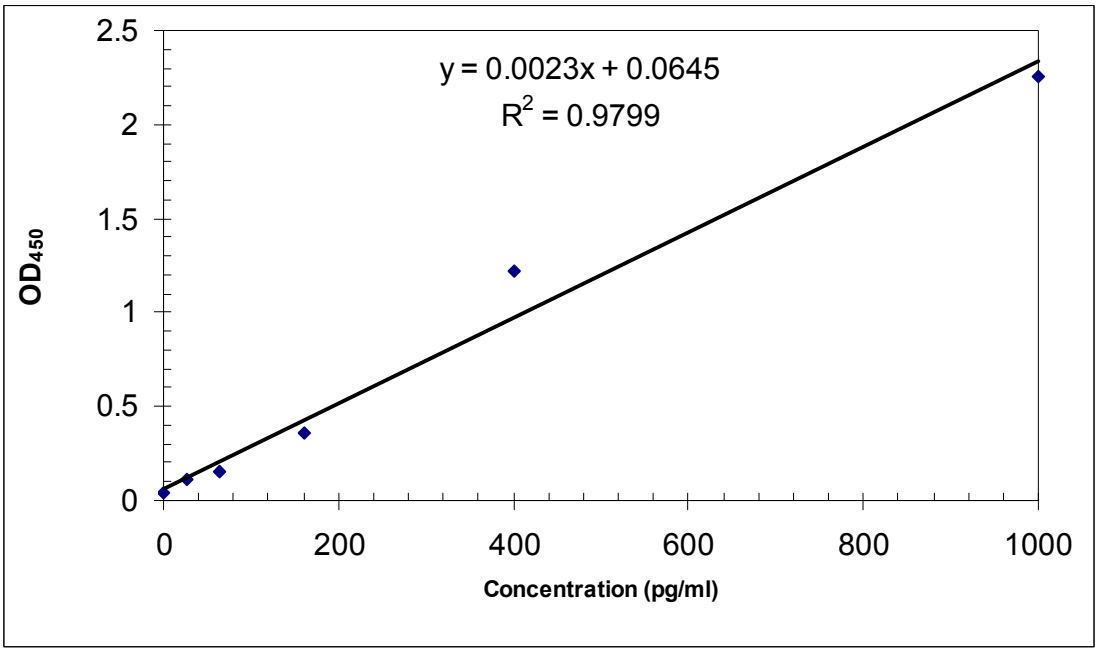

Figure 4 IFN-γ Sample Standard Curve.

2.7 Human TNF-α

The initial setup was identical to that used for IFN-γ (section 2.6). After the samples, standards, and RPMI 10% FBS were added to their respective wells, the plate coated with anti-TNF-α was sealed with a plate sealer and incubated at 37˚C for 2 hours. The contents were discarded by inversion and each well was washed four times with wash buffer. Anti-TNF-α was added to each well except the blank following incubation. The plate was sealed and incubated at 37˚C for one hour.

Following incubation, the contents were discarded and each well was washed four times. Conjugate was added to each well and the plates were sealed and incubated at 37˚C for 30 minutes. Contents were once again emptied and wells were washed four times. Substrate was added to each well and the plate was sealed and incubated at room temperature for 30 minutes. Following incubation, stop solution

was added to each well and the plate was again incubated at room temperature for 30 minutes. The plate reader was blanked against the blank wells and readings were taken at 450nm with correction at 570 and 590nm. The concentration was determined by extrapolation from the standard curve. All ratios were run in duplicate and averaged prior to graphing. In addition, a blank well with RPMI with 10% FBS was subtracted from all ratios.

2.8 Isolation of Eristostatin

Eristostatin was synthesized as a recombinant protein in *Escherichia coli* BL21 using a modified pET32b plasmid with a kanamycin resistance gene. One well isolated colony was then added to (15µg/mL) kanamycin-treated LB broth and incubated overnight at 37˚C at 250rpm.

The following day, the broth with growth was diluted with fresh kanamycin-treated LB broth and incubated for 3 hours at 250rpm. Isopropyl-beta-D-thiogalactopyranoside (IPTG) (0.4mM) (Novagen, Madison, WI) was added to the broth and it was incubated for 3 hours at 250rpm. The broth was transferred into centrifuge bottles and centrifuged for 10 minutes at 3900g. The supernatant was decanted and the pellet was stored at -80˚C overnight.

Pellets were thawed at room temperature for an hour. Lysis buffer was added (1x binding buffer with 0.1% Tergitol-type nonyl phenoxylpolyethoxylethanol-40 (NP40)) and the bottles were incubated at room temperature for 15 minutes. The viscous product was sonicated on ice at 80-90 % four times for two minutes each with a 15 second interval between each sonication. The sonicate was inverted two times and put back on the sonicator at the same setting two times for two minutes each with a 15 second interval between each run. The sonicate was centrifuged at 28,955g for

20 minutes. Finally, the supernatant was filtered using a 0.45µ syringe filter, the pellet was removed and discarded.

A His-bind column from Novagen (USA) was washed with strip buffer from Novagen (Madison, WI) then distilled water. Charge buffer from Novagen (Madison, WI) was added to the column followed by equilibration with binding buffer from Novagen (Madison, WI). The cell extract was filtered through a 0.22µ Steriflip from Millipore (Billerica, Massachusetts) and added to the column. The column was washed with binding buffer. Thrombin (1000 units/mg) (Novagen, Madison, WI) was added. The bottom of the column was closed and binding buffer was added. The column was left at 4˚C overnight. Two fractions were collected and acetonitrile gradient High Performance Liquid Chromatography (HPLC) (Agilent HPLC 1100, Agilent Technologies, Santa Clara, CA) was used to isolate the recombinant eristostatin.

Chapter 3

RESULTS

3.1 IFN-γ Expression

SbCl2 and MV3 did not show a significant increase in IFN-γ levels as the E:T ratio increased (Figures 5 and 6). It should be noted that the IFN-γ cytokine experiment was only done once for SbCl2 and MV3. Therefore, error bars are not applicable.

For all E:T ratios in the MV3 experiment, the IFN-γ concentrations for both the control and the eristostatin-treated cells never reached levels greater than 20pg/mL and reached a minimum concentration of zero pg/mL (Figure 5). Concentrations below the detection threshold where the absorbance in the blank well with fresh RPMI with 10% FBS exceeded the test absorbance value were assigned a concentration of zero pg/mL. Furthermore, this experiment was done only once and the data must be interpreted with caution. The zero E:T ratio (only melanoma cells) the concentration of IFN-γ was found to be 20pg/mL with the eristostatin-treated cells and zero pg/mL for the control. For the higher E:T ratios of ten and five, the eristostatin-treated cells yielded higher IFN-γ than the control. However, at the one E:T ratio, the control yielded a higher IFN-γ concentration.

Like MV3, SbCl2 yielded low concentrations of IFN-γ across all ratios, such that the highest concentration obtained was 27pg/mL and the lowest concentration obtained was below the level of detection and considered zero pg/mL (Figure 6). The trend, however, is the complete opposite of that shown by MV3. At the zero and ten E:T ratios, the control showed higher IFN-γ concentrations than the

eristostatin-treated cells and lower IFN-γ concentrations at the other ratios between. Both of these cell lines showed an overall alternating trend between eristostatin and the control, almost resembling two sine curves offset by 180° (Figure 7). It is important to note that this study was done only once and a pipetting error may have occurred at the ten E:T ratio of the eristostatin-treated cells.

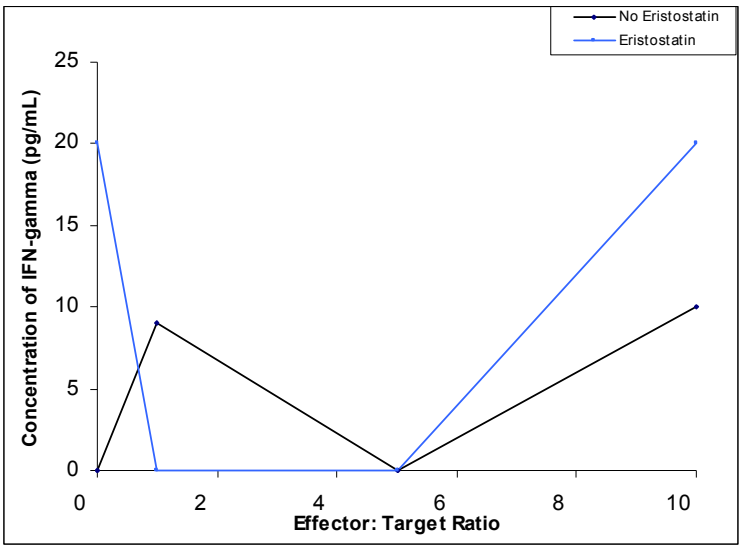

Figure 5 **Concentration of IFN-γ versus Effector (Natural Killer cells): Target (MV3) Ratio.**

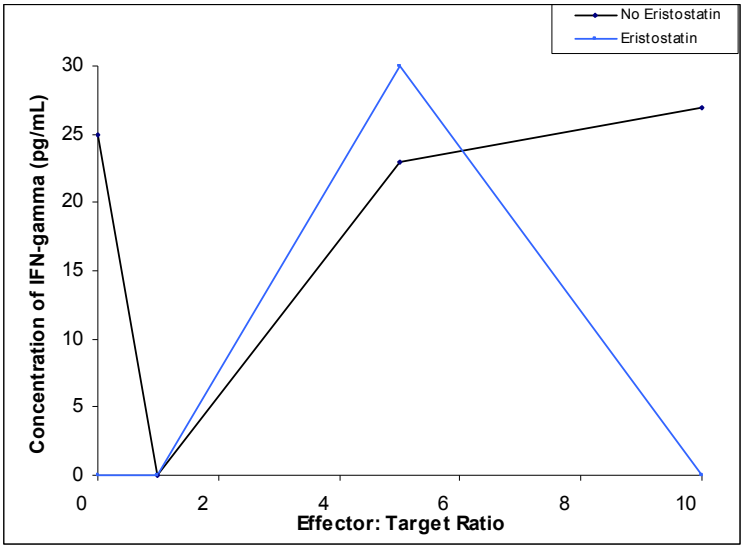

Figure 6 **Concentration of IFN-γ versus Effector (Natural Killer cells): Target (SbCl2) Ratio.**

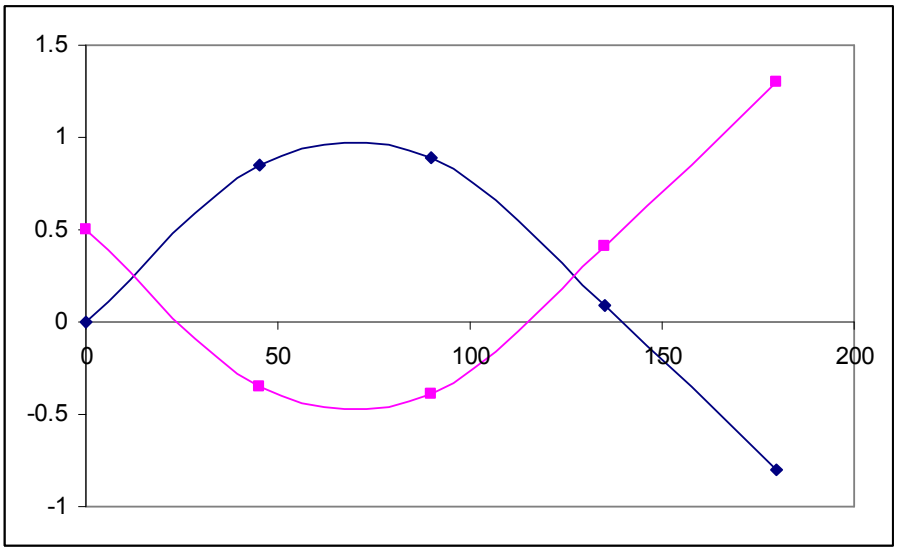

Figure 7 **Two Classic Sine Functions Offset By 180°.** The two functions above show an alternating pattern also seen with the IFN-γ data.

Unlike MV3 and SbCl2, M24met yielded significantly higher IFN-γ concentrations with a highest concentration of 1468pg/mL in the control at the ten E:T ratio in run#2. Whether run #2 had an outlier is unclear, and the data is presented in raw form (Tables 1 and 2) and as an average of both runs (Figure 8). Run #1 also showed elevated levels of IFN-γ yielding a highest IFN-γ concentration of 81pg/mL at the 10 E:T eristostatin-treated ratio. The error bars for M24met in Figure 8 suggest a trend were no difference exists between eristostatin and the control in spite of the higher average for the control. The alternating pattern seen with SbCl2 and MV3 is also evident with M24met (Figure 9).

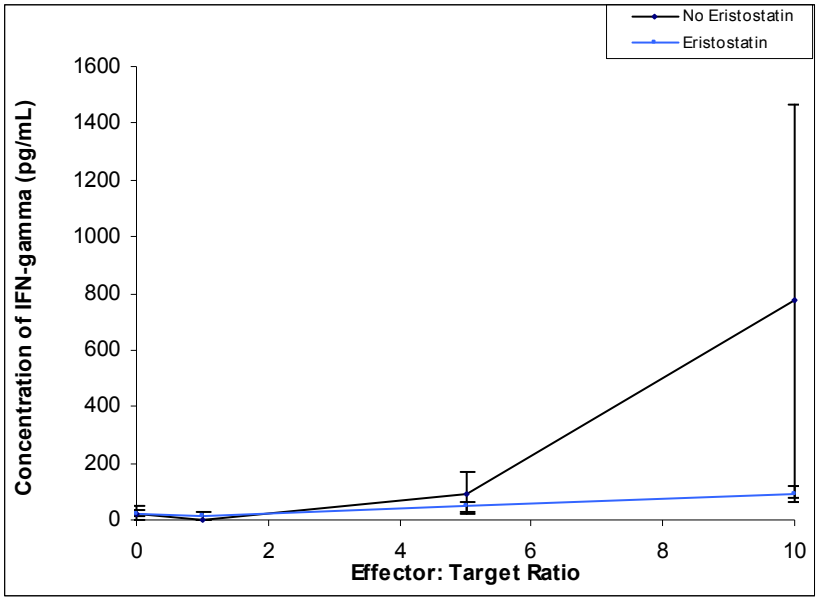

Figure 8 **Average Concentration of IFN-γ versus Effector (Natural Killer cells):Target (M24met) Ratio.**

Effector:Target ratio	Control IFN-γ (pg/mL)	standard error (stdev/(n^0.5))	Eristostatin IFN-γ (pg/mL)	standard error (stdev/(n^0.5))
0	24.5	12.5	14	33
1	0	3	13	12
5	94	72	47	18
10	774.5	693.5	91.5	25.5

Table 1 **Effector (NK cells): Target (M24met) Ratio and average IFN-γ Concentrations with Associated Standard Error.** The green highlight points to the high standard error due to the suspected outlier.

M24met Run #1		
E:T Ratio	Control IFN-γ (pg/mL)	Eristostatin IFN-γ (pg/mL)
0	12	0
1	0	25
5	22	65
10	81	66
M24met Run #2		
E:T ratio	Control IFN-γ (pg/mL)	Eristostatin IFN-γ (pg/mL)
0	37	47
1	0	1
5	166	29
10	1468	117

Table 2 **Raw Data Results for Effector (NK cells): Target (M24met) and Associated IFN-γ Concentrations.**

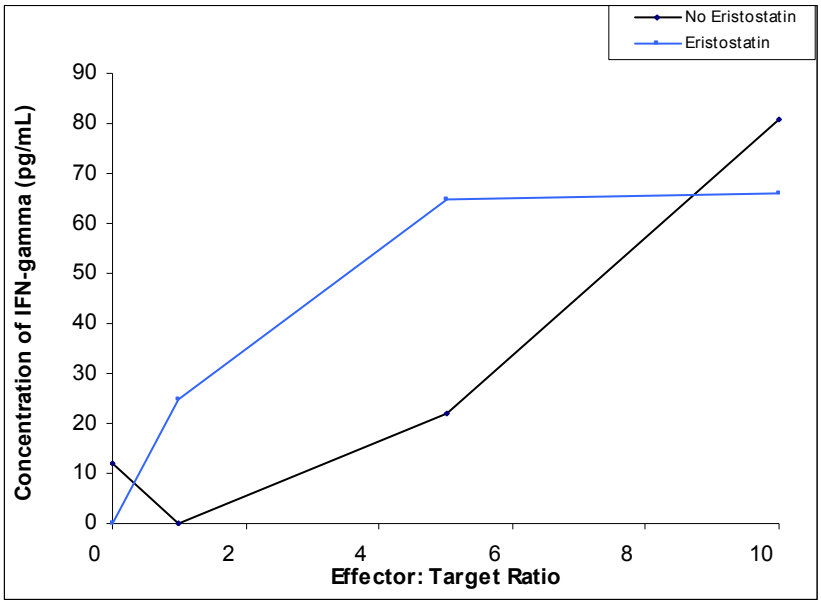

Figure 9 **Concentration of IFN-γ versus Effector (Natural Killer cells):Target (M24met) Ratio of Run#1.**

1205Lu, unlike the other cell lines, showed a notable increase in IFN-γ with eristostatin-treated cells over the control. The eristostatin-treated cells at the ten E:T ratio showed IFN-γ levels up to 466pg/mL while the control reached a maximum of 64pg/mL in the three experiments that were carried out. At the ten E:T ratio, the standard errors suggest a trend were there is a notable difference in IFN-γ concentration between the eristostatin-treated cells and the control (Figure 10). This conclusion cannot be made about the other ratios.

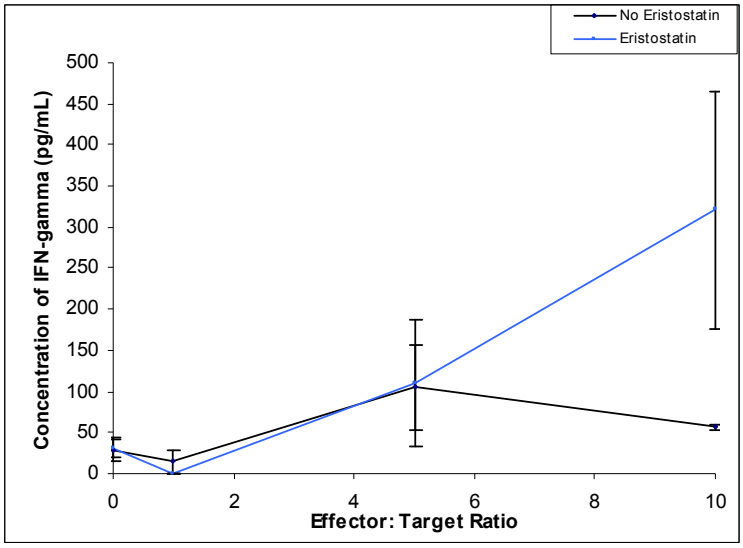

Figure 10 **Concentration of IFN-γ versus Effector (Natural Killer cells):Target (1205Lu).** Data is representative of two assays and standard error is shown.

3.2 TNF-α Expression

SbCl2, MV3, M24met, and 1205Lu maintained low levels of TNF-α as E:T ratios increased when treated with eristostatin. The same pattern was also evident in the controls. It must be noted that the experiments were only done once (i.e. n=1) and therefore, error bars are not applicable.

Levels of TNF-α remained below 60pg/mL for all cell lines at all ratios. In addition, a general upward trend is evident in all the tested cell lines with exception of a few data points and SbCl2 which seemed low across all ratios (Figure 11). It is also evident that at the zero E:T ratio (containing only melanoma cells), TNF-α concentrations were higher in the eristostatin-treated cells compared to the controls (Figure 11, 12, 13, and 14).

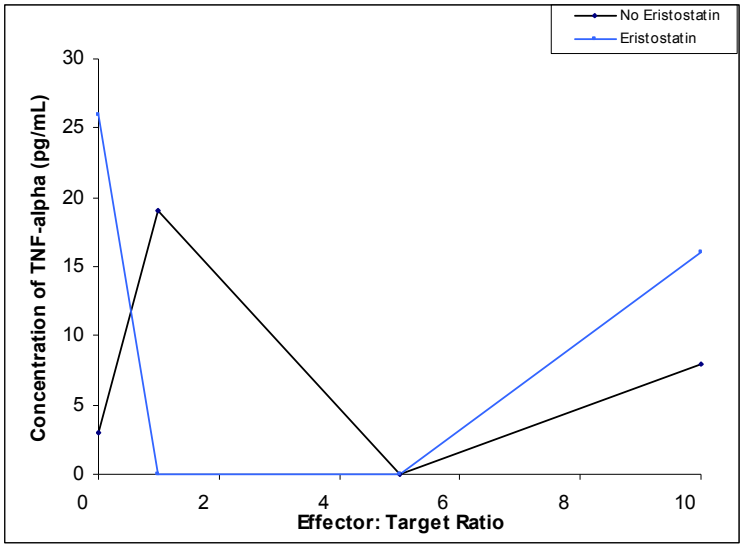

Figure 11 Concentration of TNF-α versus Effector (NK cells):Target (SbCl2).

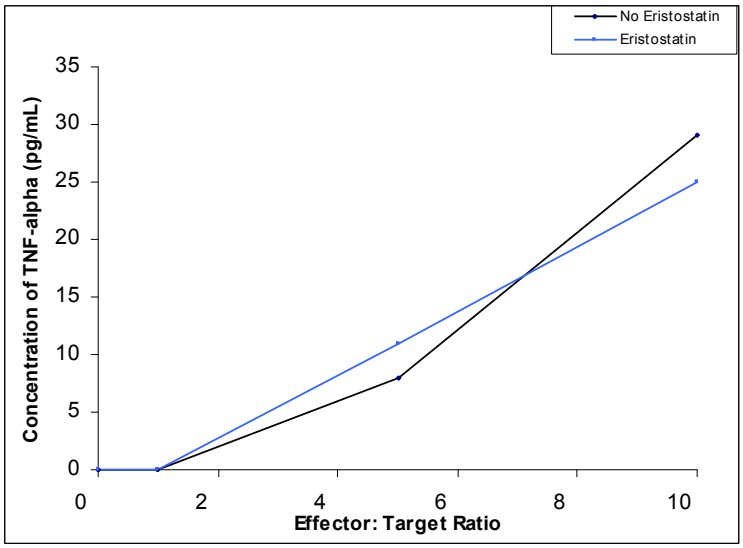

Figure 12 Concentration of TNF-α versus Effector (NK cells):Target (MV3).

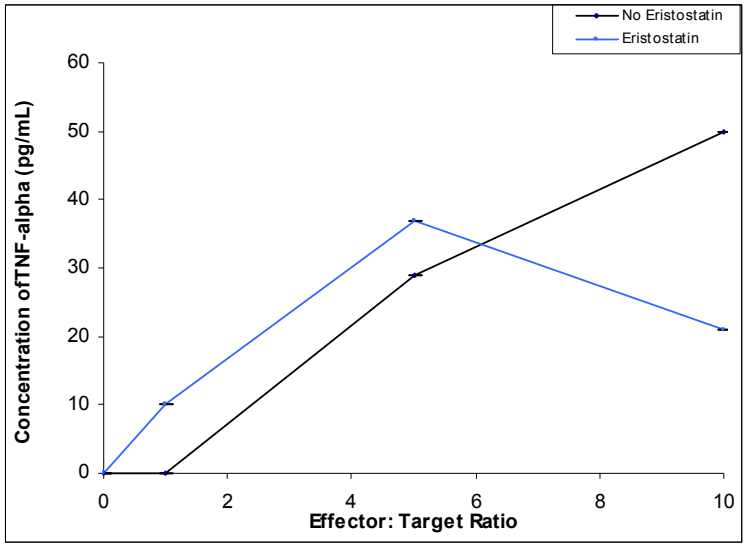

Figure 13 **Concentration of TNF-α versus Effector (NK cells):Target (M24met).**

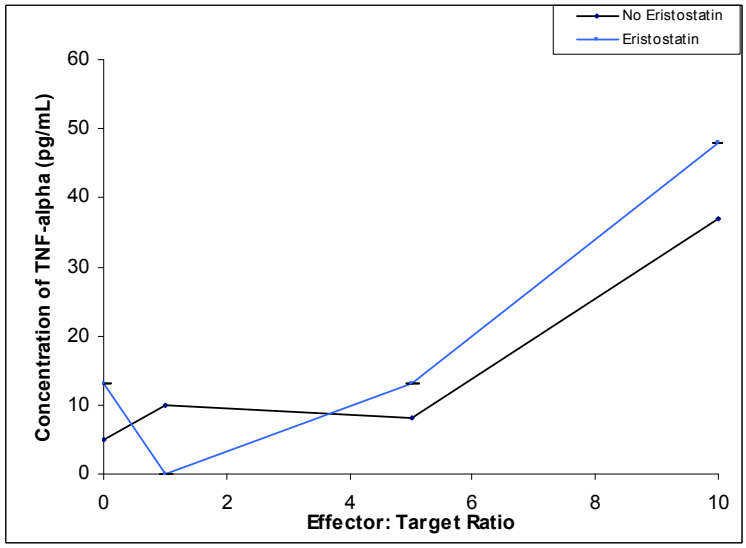

Figure 14 **Concentration of TNF-α versus Effector (NK cells): Target (1205Lu).**

3.3 CytoTox-Glo Cytotoxicity

Cytotoxicity data is conventionally presented as present lysis after the background is subtracted. However, this conventional methodology assumes that the background is identical with and without the substance of interest. In other terms, by subtracting background, one assumes that survivability is identical between the eristostatin-treated cells and the control cells. However, in this study, it was found that eristostatin does have an impact on survivability of melanoma cells after a short incubation. Therefore, it was deemed necessary to present the background data as well as conventional methodologies. Conventional methodologies grant information about the effects of eristostatin on the ability of NK cells to lyse melanoma cells while the background data provides information about cell survivability.

After subtracting the luminescence of the zero E:T ratio (just melanoma cells) of the eristostatin-treated cells from the luminescence of all the other ratios of eristostatin-treated cells and subtracting the zero E:T ratio luminescence of the control from all the control ratios, a modified percent lysis curve was created to help minimize the intrinsic effect of eristostatin on melanoma cell survivability. The adjusted graph does not show a notable difference between the eristostatin-treated cells and the control (Figure 15). For the one and five E:T ratio the control yielded a higher percent lysis than the eristostatin-treated cells (Figure 15). However, the trend reverses at the ten E:T ratio. The 1205Lu experiment was repeated three times (n=3).

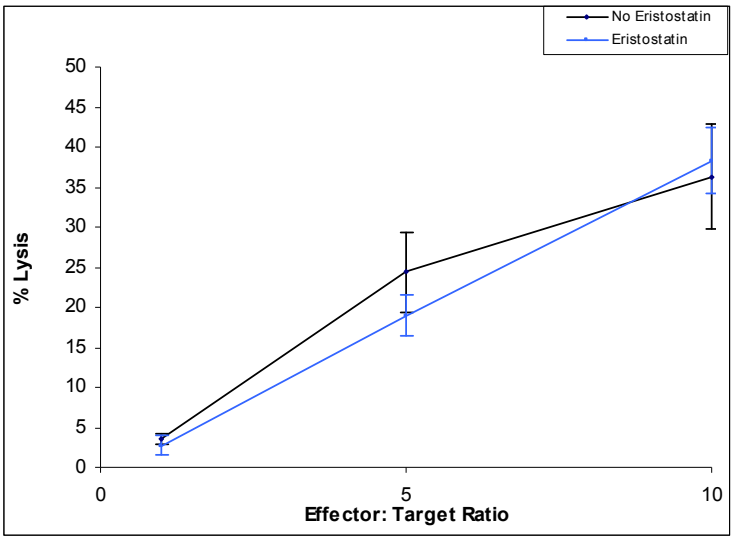

Figure 15 CytoTox-Glo Adjusted Percent Lysis versus Effector (NK cells): Target (1205Lu) Ratio.

C8161 showed a trend that differed from 1205Lu. At all ratios, the control showed a higher percent lysis on average than the eristostatin-treated cells (Figure 16). The error bars suggest that this difference was notable at only the one E:T ratio. The experiment was done in duplicate for C8161 (n=2). A maximum percent lysis of 63% was obtained with the control at the ten E:T ratio.

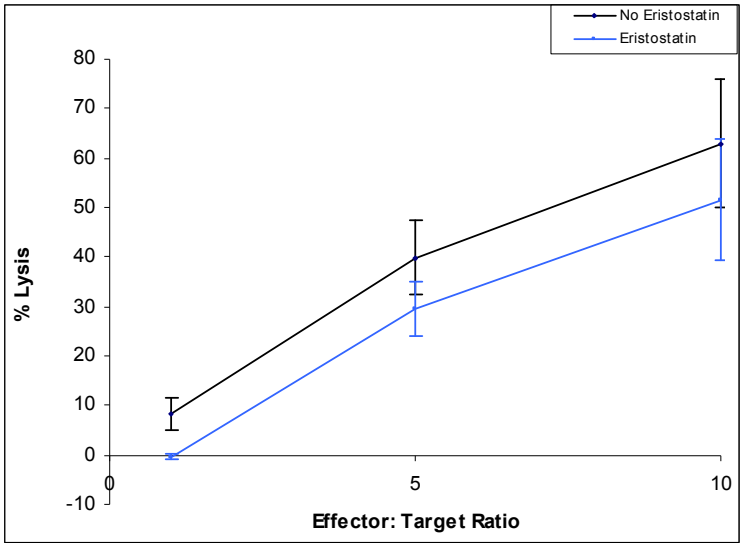

Figure 16 CytoTox-Glo Adjusted Percent Lysis versus Effector (NK cells): Target (C8161) Ratio.

M24met showed a pattern that differed from C8161 and 1205Lu. At the one and five E:T ratios, the control yielded a higher percent lysis than the eristostatin-treated cells. At the ten E:T ratio, the eristostatin-treated cells showed a higher percent lysis (Figure 17). It is not known whether this difference was significant according to the standard error bars since the experiment was done only once. The maximum lysis achieved was 66% at the ten E:T ratio of the eristostatin-treated cells.

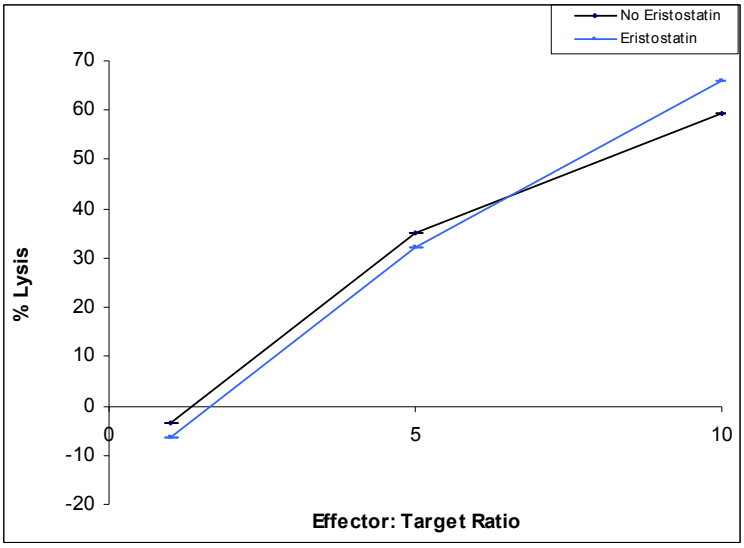

Figure 17 CytoTox-Glo Adjusted Percent Lysis versus Effector (NK cells): Target (M24met) Ratio.

Just like M24met, a cytotoxicity assay using WM164 was done only once. Therefore, errors bars do not apply for this cell line. The trend suggested by this cell line resembles those presented earlier where the control displayed a lower percent lysis than the eristostatin-treated cells at the five and ten E:T ratios. However, at the one E:T ratio, the percent lysis is nearly identical for the control and eristostatin run (Figure 18). The maximum percent lysis achieved was 61% by the control at the ten E:T ratio.

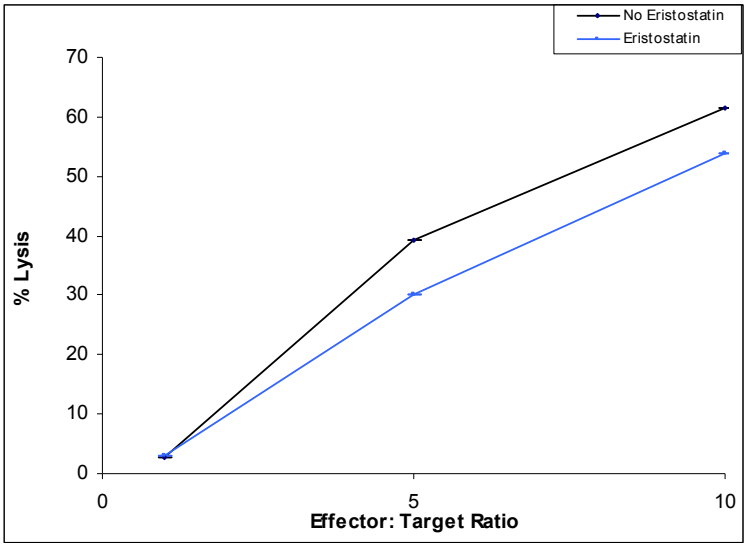

Figure 18 CytoTox-Glo Adjusted Percent Lysis versus Effector (NK cells): Target (WM164) Ratio.

The background data for CytoTox-Glo suggested that the eristostatin-treated 1205Lu cells alone had a 4.37% higher percent lysis than the control 1205Lu cells. Furthermore, the difference was notable according to the error bars (Figure 19). This conclusion cannot be made about the other tested cell lines. For C8161, the control yielded a 2.5% higher initial lysis than the eristostatin-treated cells although the error bars do not conclusively support this trend (Figure 19). The percent lysis did not differ significantly between the control and the eristostatin-treated cells showing a difference of only 0.5% lysis for M24met (Figure 19). For WM164, the control showed a 1.7% higher initial lysis than the eristostatin-treated cells (Figure 19).

.

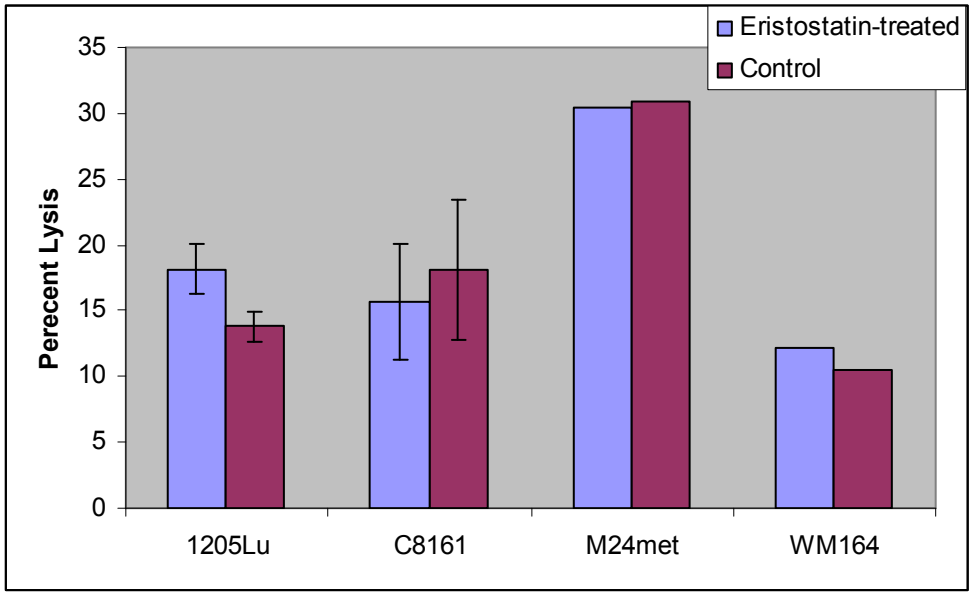

Figure 19 Background Percent Lysis using CytoTox-Glo.

3.4 Flow Cytometric Cytotoxicity

Using flow cytometry, for 1205Lu it is evident that the control on average had a higher percent lysis than the eristostatin-treated cells at all E:T ratios although the difference was not notable according to the standard error bars (Figure 20). The experiment was repeated four times and achieved a maximum percent lysis of 9.2% at the five E:T ratio of the control.

Like 1205Lu, the C8161 control also showed a higher percent lysis than the eristostatin-treated cells at nearly all E:T ratios. The only exception was the 2.5 E:T ratio where the eristostatin-treated cells yielded a higher percent lysis. The difference was notable according to the standard error bars at only the 10 E:T ratio (Figure 21). A maximum percent lysis of 13% was achieved at the ten E:T ratio of the control.

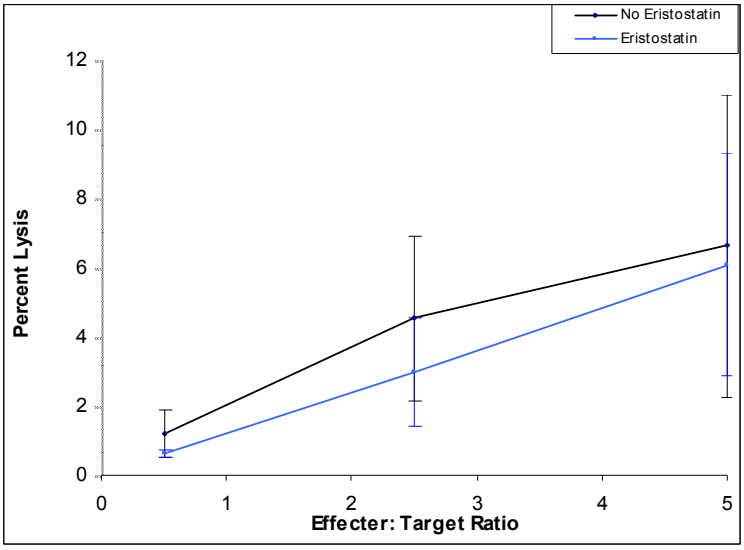

Figure 20 **Flow Cytometry Adjusted Percent Lysis versus Effector (NK cells): Target (1205Lu) Ratio.**

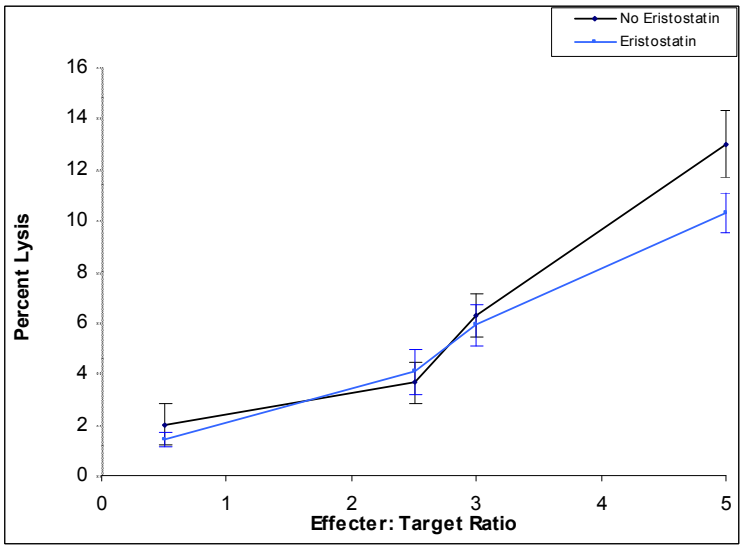

Figure 21 **Flow Cytometry Adjusted Percent Lysis versus Effector (NK cells): Target (C8161) Ratio**.

Unlike 1205Lu and C8161 in which the experiments were repeated four and three times respectively, M24met was done only once. Obvious trends are not as evident in this run. However, it is important to note that at all ratios except the ten E:T ratio, the eristostatin-treated cells yield a higher percent lysis than the control (Figure 22). A maximum percent lysis of 8.1% was achieved at the five E:T ratio of the eristostatin-treated cells.

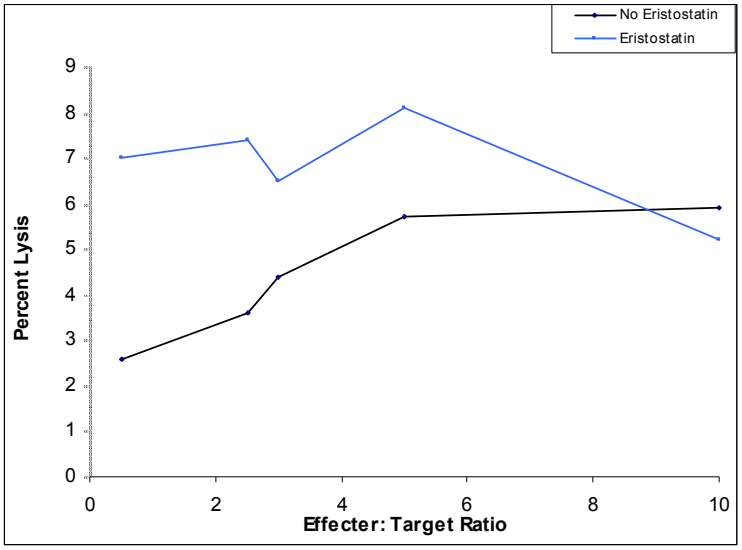

Figure 22 Flow Cytometry Adjusted Percent Lysis versus Effector (NK cells): Target (M24met) Ratio.

WM164 yielded a lower percent lysis when compared to the other cell lines reaching a maximum of 0.67% lysis at the 0.5 E:T ratio of the eristostain treated cells. The control was higher the eristostatin-treated cells with all ratios except the 0.5 E:T ratio (Figure 23). The standard error suggest that the finding that eristostatin-treated cells present with a higher percent lysis at the 0.5 E:T ratio is notable. The

percent lysis on the adjusted graph went below zero because the zero E:T ratio (just melanoma cells) percent lysis was higher than some of the other ratios. WM164 was repeated three times.

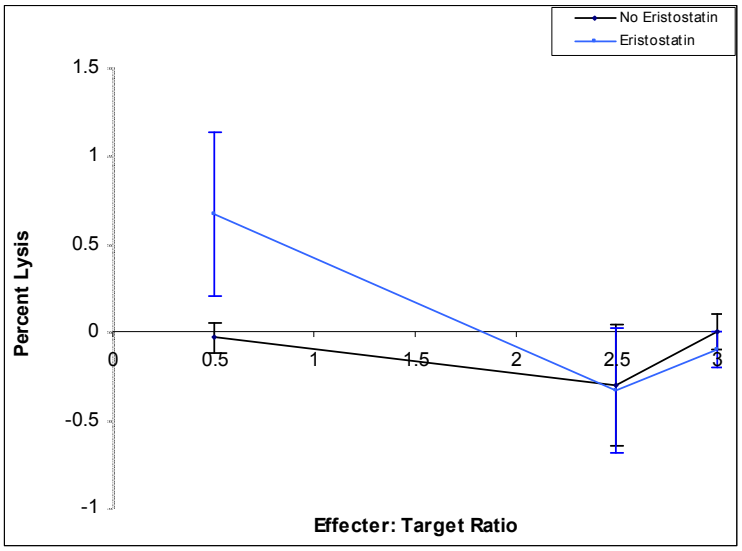

Figure 23 Flow Cytometry Adjusted Percent Lysis versus Effector (NK cells): Target (WM164) Ratio.

MV3 showed a similar pattern to M24met. All ratios yielded a higher percent lysis in the controls compared to the eristostatin-treated cells except at the 2.5 E:T ratio. None of the differences seen are notable according to the standard error bars (Figure 24). MV3 was repeated at total of four times. A maximum percent lysis of 9.2% was achieved at the five E:T ratio of the control.

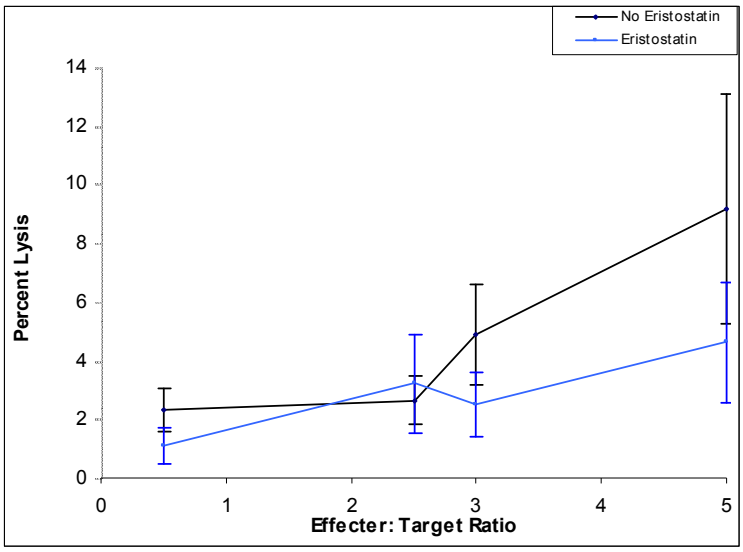

Figure 24 Flow Cytometry Adjusted Percent Lysis versus Effector (NK cells): Target (MV3) Ratio.

SbCl2 was done in duplicate. Unlike any of the other cell lines, on average, the eristostatin-treated cells showed a higher percent lysis than the controls at all ratios. This difference was notable according to the standard error at the 2.5 E:T ratio (Figure 25).

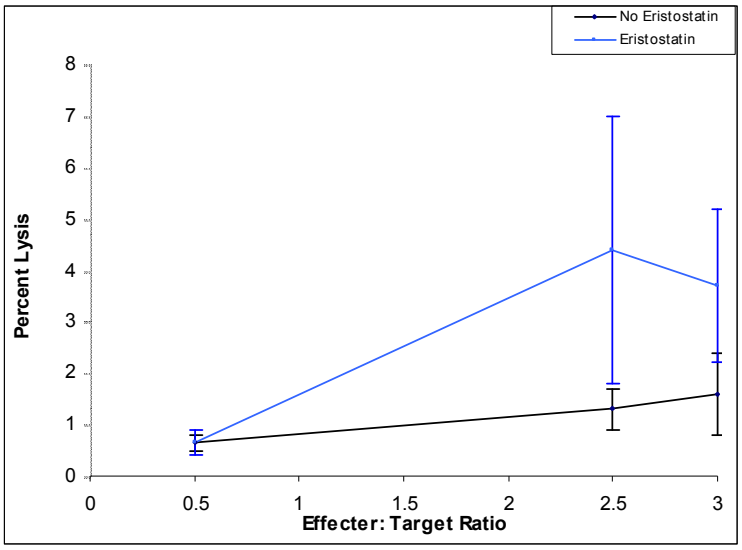

Figure 25 Flow Cytometry Adjusted Percent Lysis versus Effector (NK cells): Target (SbCl2) Ratio.

The background data for the Flow Cytometric Cytotoxicity Assay suggested important trends. With all tested cell lines except SbCl2, the control showed a higher percent lysis than the eristostatin-treated cells (Figure 26). According to the standard error bars, this difference was notable with 1205Lu and C8161. Furthermore, the difference for M24met was pronounced although the experiment was done only once. For SbCl2, the eristostatin-treated cells yielded a slightly higher percent lysis than the control. However, the error bars suggest that this difference is not notable (Figure 26).

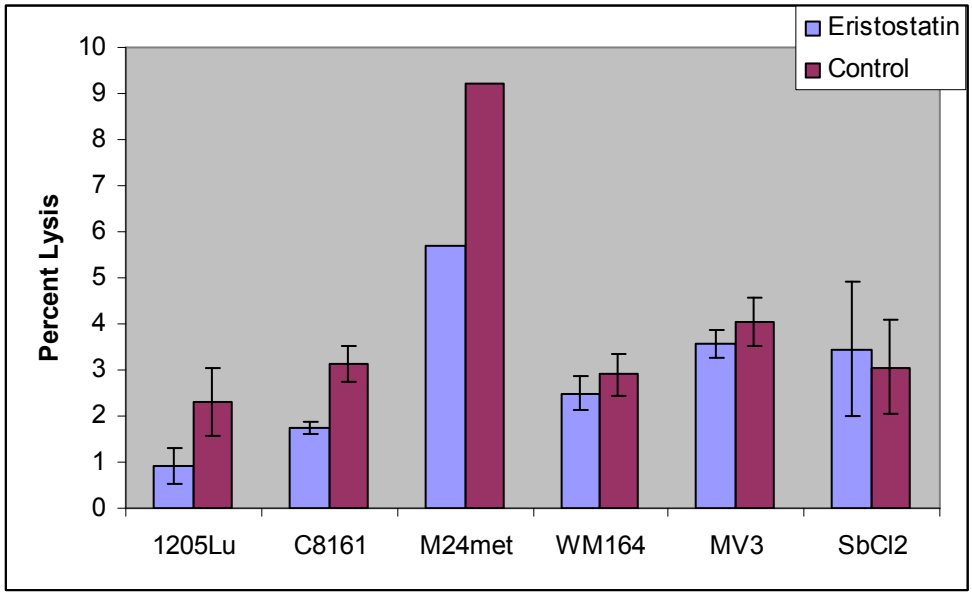

Figure 26 Background Data Using Flow Cytometric Cytotoxicity Assay

3.5 Assessment of NK Purity

Following isolation of NK cells from a donor, NK cells were stained with mouse IgG anti-human CD56 and an mouse IgG-2a isotype control to determine purity via flow cytometry. For all purity checks, NK cells were over 90% pure. One example is shown in Figure 27 (unstained), 28 (isotype control), and 29 (stained with FITC-labeled anti-CD56). The isotype control was negative and the isolated population was 97.1% pure (Figure 29).

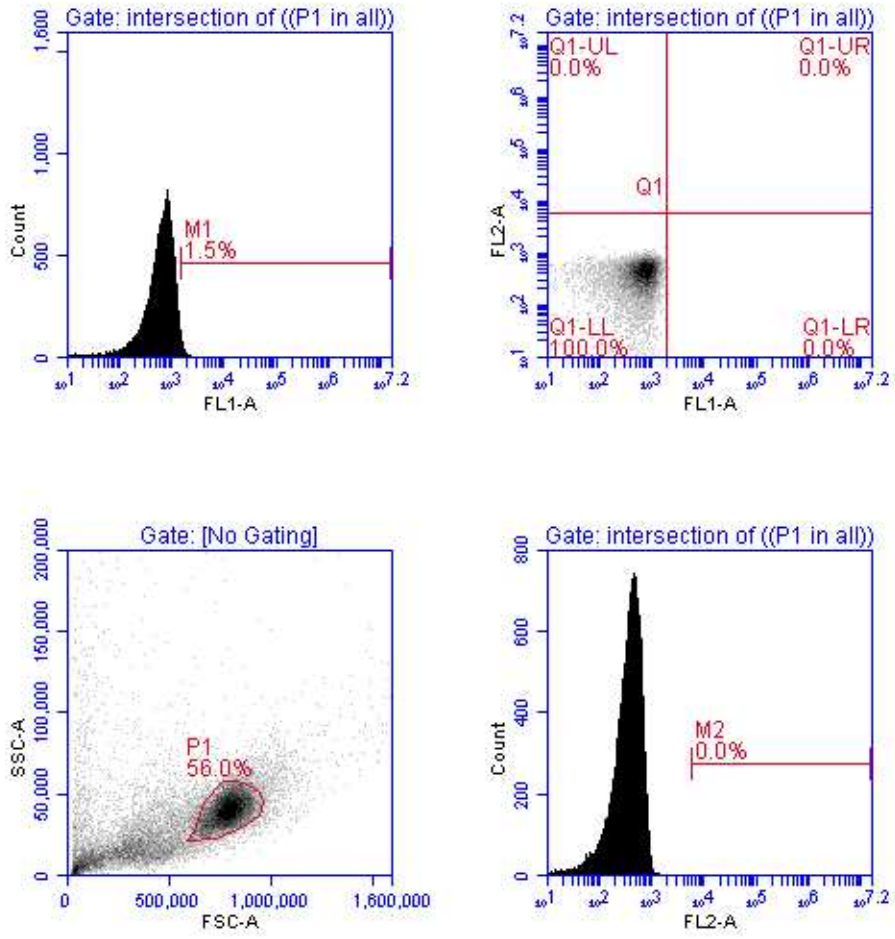

Figure 27 **Unstained Natural Killer cells in Natural Killer Purity Study via Flow Cytometry.** Top left histogram: used to set negative fluorescence for FL1-A, the FITC marker tagged to Anit-CD56 and the isotype control. Bottom left: the gate (P1) used for NK cells. The top right: density plot after negative values were set for FL1-A and FL2-A. Bottom right: FL2-A, propidium iodide, histogram.

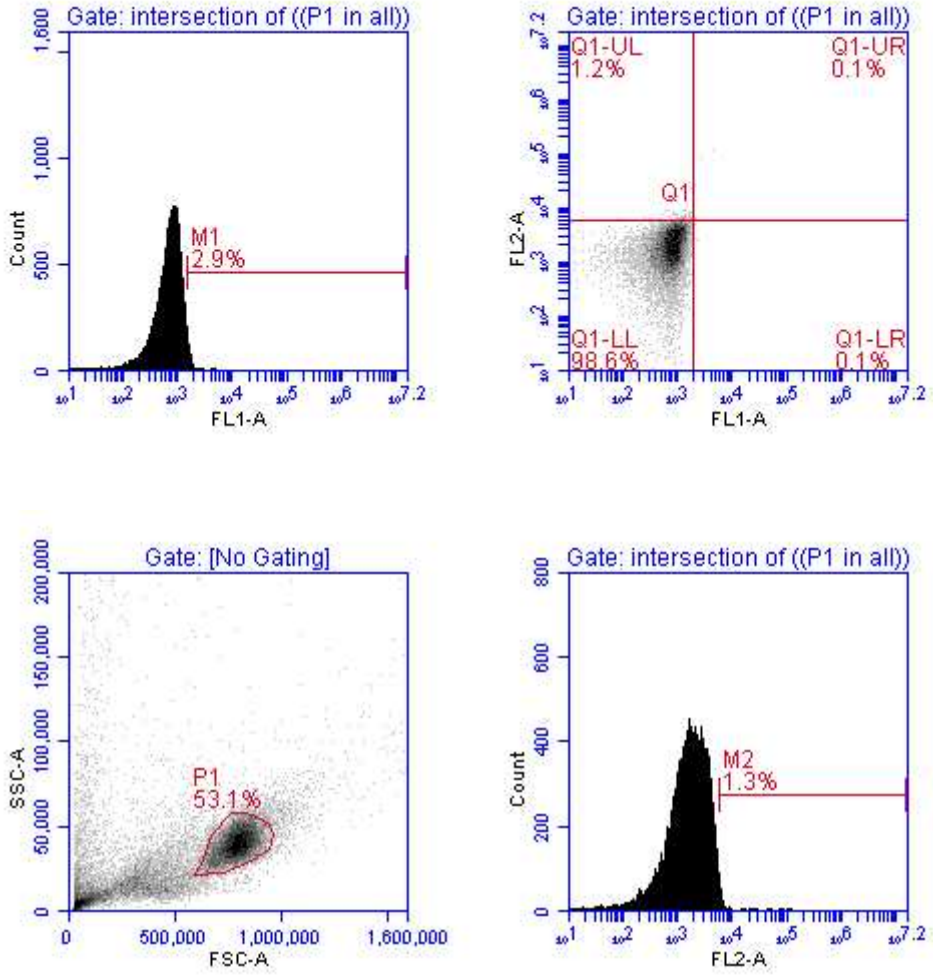

Figure 28 **Isotype Control Stained Natural Killer cells in Natural Killer Purity Study via Flow Cytometry.** Top left: histogram used to set negative fluorescence for FL2-A, the propidium iodide fluorescence channel. Bottom left: gate (P1) used for NK cells. Top right: density plot after negative values are set for FL1-A and FL2-A. The cells were negative in the isotype control. Bottom right: FL2-A, propidium iodide, histogram.

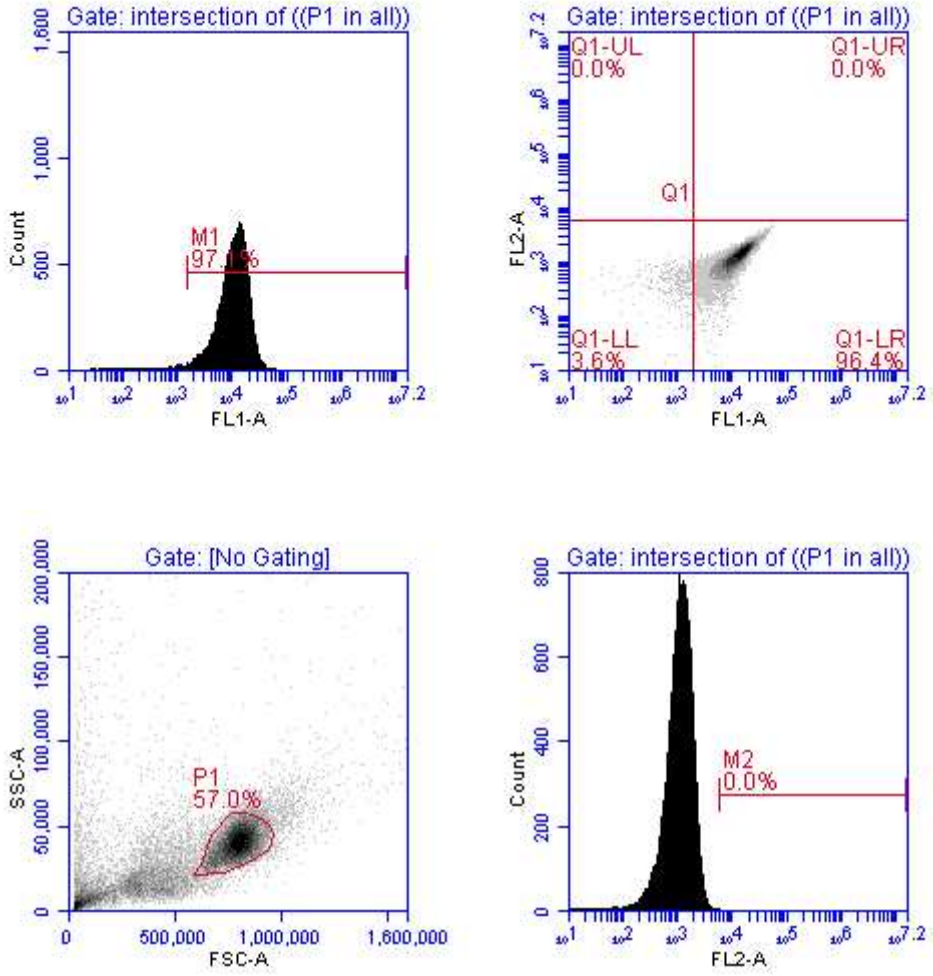

Figure 29 **Anti-CD56 Stained Isotype Natural Killer cells in Natural Killer Purity Study via Flow Cytometry.** Top left: histogram used to determine purity. Top right: density plot after negative values are set for FL1-A and FL2-A. The cells are positive for FL1-A, the anti-CD56 marker. The bottom left hand graph shows the gates used for NK cells. Bottom right: FL-2, propidium iodide, histogram.

3.6 Three Dimensional Results

Only C8161 was tested using the laminin-rich Matrigel® 3D matrix media. The experiment was performed twice. On day one (Figures 30 and 31), it is evident that the growth patterns lack the complexity seen on day three (Figures 39). In addition, most cells are negative for propidium iodide which suggested minimal cell death. The eristostatin-treated cells and the control showed no difference in spatial configuration, complexity, or cell survivability.

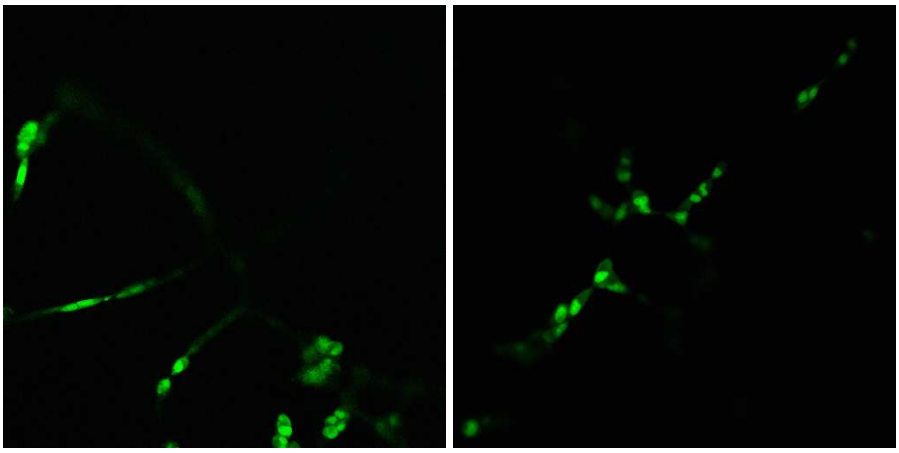

Figure 30 Confocal Microscopy Images of C8161 Control on Day One at 200x Stained with Nuclear Stain, Syto (green).

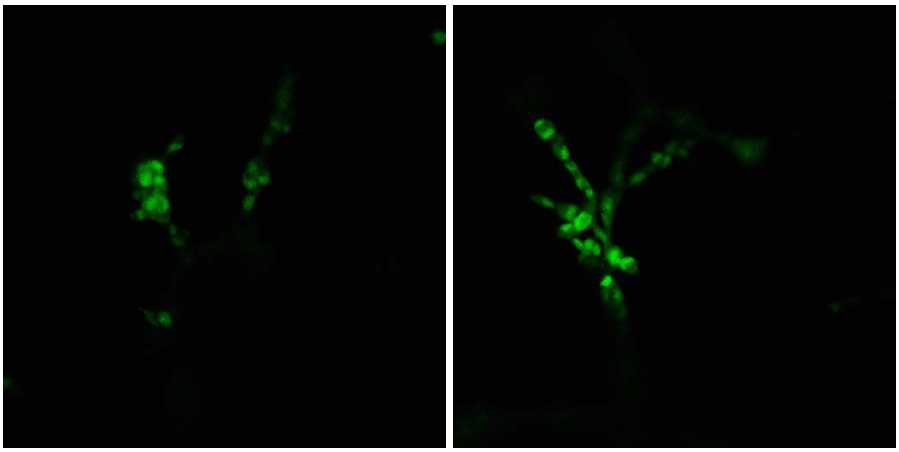

Figure 31 Confocal Microscopy Images of Eristostatin-treated C8161 on Day One at 200x Stained with Nuclear Stain, Syto (green).

On day three, more complex structures were evident including two banana-shaped structures present in the eristostain-treated wells and the control wells (Figure 38). As seen in day one, no apparent differences existed between the control and the eristostatin-treated wells (Figure 32-38). The number of dead cells was similar and there were no apparent spatial configuration differences.

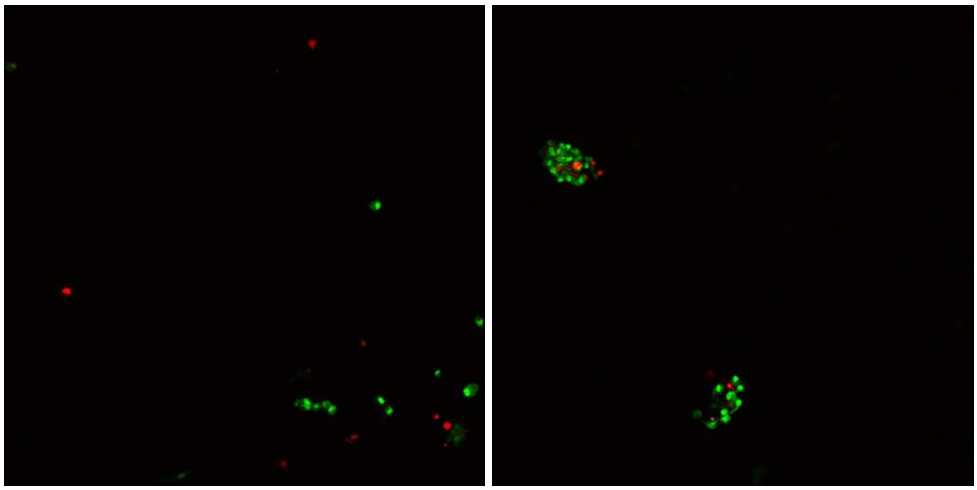

Figure 32 **Confocal Microscopy Images of C8161 Control on Day Three at 100x Stained with Syto (green) and Propidium Iodide (red).** Images were taken in center of well.

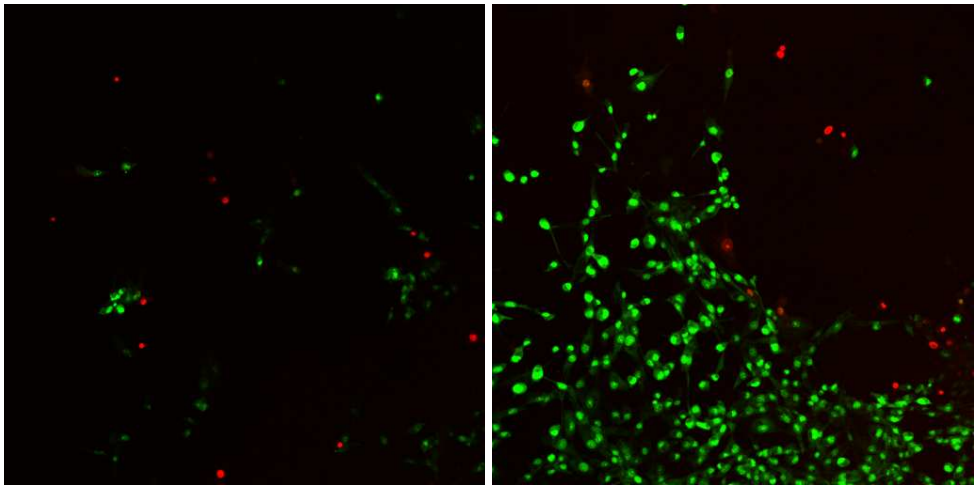

Figure 33 **Confocal Microscopy Images of Eristostatin-treated C8161 on Day Three at 100x Stained with Syto (green) and Propidium Iodide(red).** The left hand image was taken in the center of the well while the right hand picture was taken on a side.

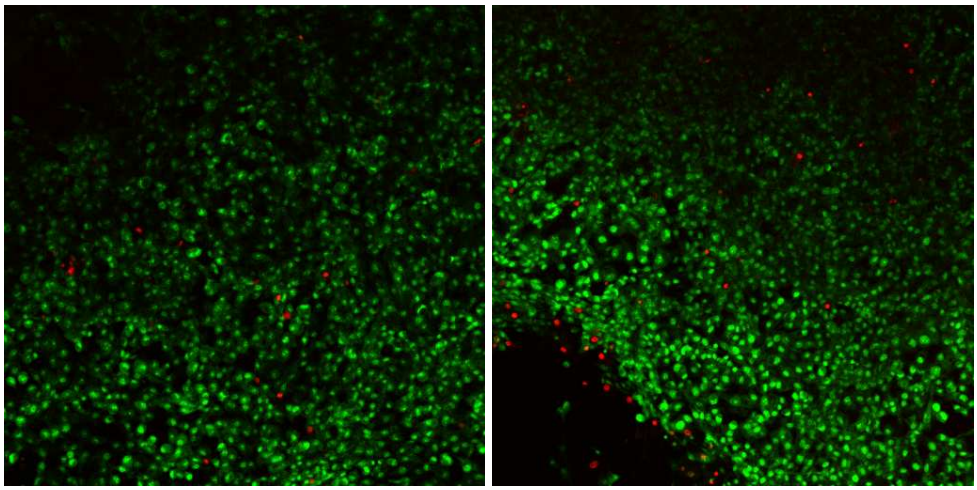

Figure 34 **Confocal Microscopy Images of C8161 Control (Left) and Eristostatin-treated (Right) on Day Three at 100x Stained with Syto (green) and Propidium Iodide (red).** Left image is control and right image is eristosatin-treated. Images were taken on side of well.

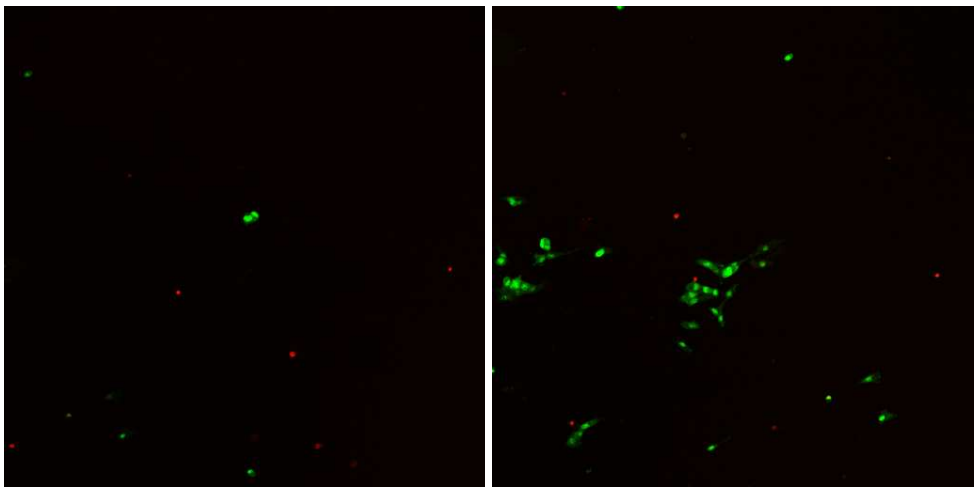

Figure 35 **Confocal Microscopy Images of C8161 Control on Day Three at 100x Stained with Syto (green) and Propidium Iodide (red).** Images were taken in the center well.

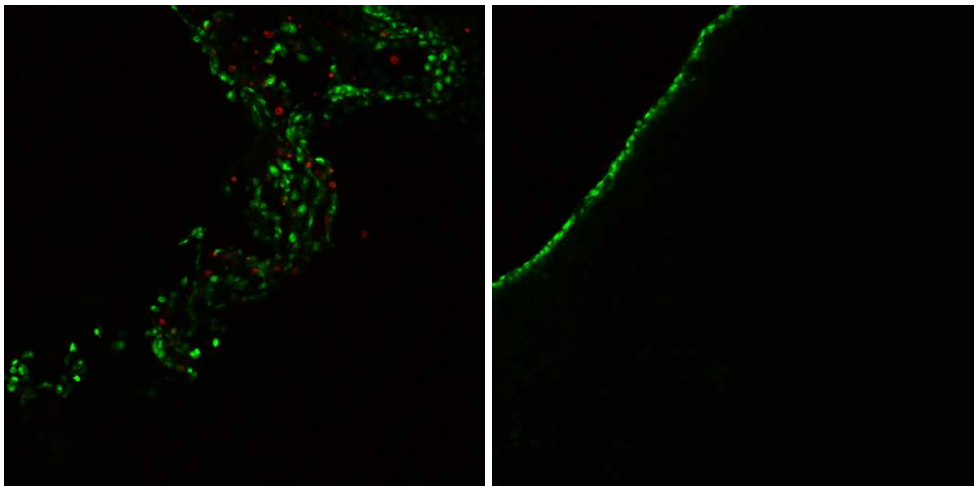

Figure 36 Confocal Microscopy Images of Eristostatin-treated C8161 on Day Three at 100x Stained with Syto (green) and Propidium Iodide (red). Image were take on side of well.

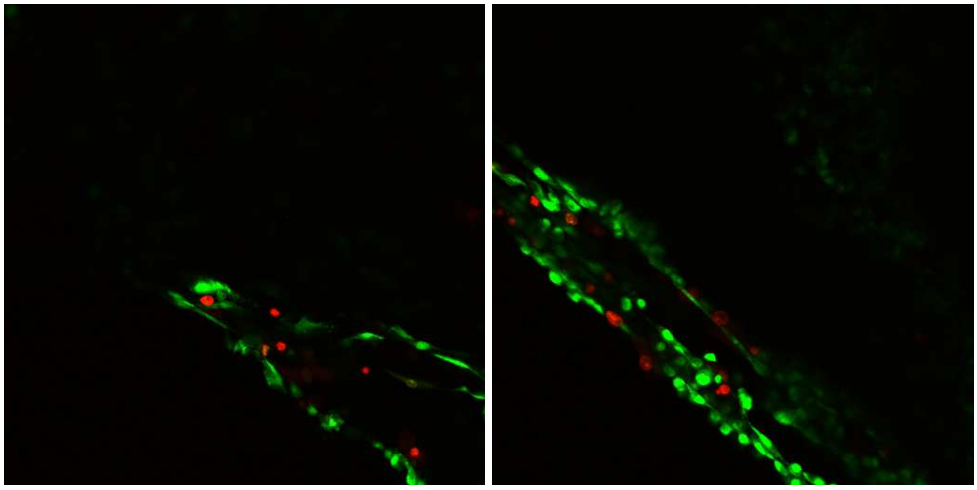

Figure 37 Confocal Microscopy Images of C8161 Control (Left) and Eristostatin-Treated (Right) on Day Three at 200x Stained with Syto (green) and Propidium Iodide (red). Image was take on side of well. Control on Left and Eristostatin treated cells on right.

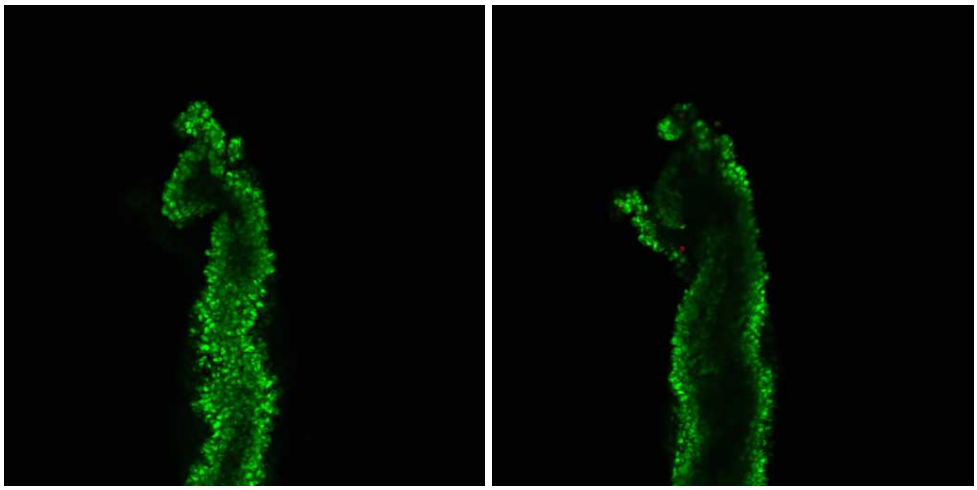

Figure 38 C8161 Banana like structures seen in Both Control and Eristostatin-treated Cells via Confocal Microscopy Images on Day Three at 100x Stained with Syto (green) and Propidium Iodide (red). Images were taken on side of well.

With the second run, various structures were seen. However, just like the first run, subjective impressions were that no apparent difference existed between the control and eristostatin-treated wells. Additional confocal images from the second run are shown (Figure 39 and 40).

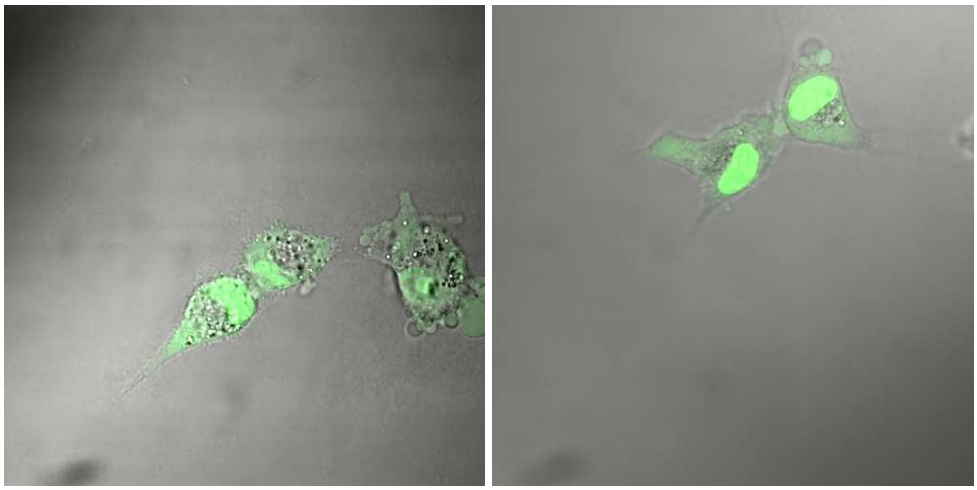

Figure 39 **Eristostatin-treated C8161 Cells via Confocal Microscopy Images 630x Stained with Syto (green) and Propidium Iodide (red) Viewed with Transmittance and Fluorescence.**

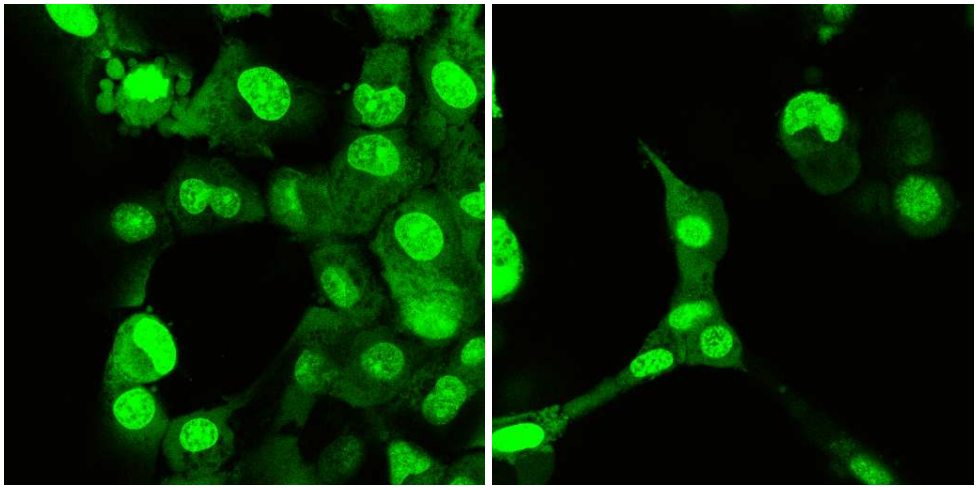

Figure 40 **Control C8161 Cells via Confocal Microscopy Images 630x Stained with Syto (green).**

Chapter 4

DISCUSSION

4.1 Points of Consideration

When assessing the experiments discussed above, it is important to note that the NK cells used in these studies came from different donors. Only volunteers who took aspirin within the past 24 hours were excluded from the study. All other donors were welcome to donate. Donors for this study were diverse in age, gender, race, and presumably fitness levels, diet, and general health.

Although these variables may seem insignificant, a few studies suggest that they may indeed be notable. Furusawa described a statistically significant decrease in NK cell cytotoxicity for paraplegic males following participation in a wheelchair marathon (Furusawa et al., 1998). Facchini noted that with age, the number of circulating NK cells increase; however, a decreased functional response is noted (Facchini et al., 1987). Facchini suggested that this increase in number may be a compensatory effect for the decreased cytolytic activity. Furthermore, in a study that compared males, females, and females on oral contraceptive, it was found that although NK cell blood concentrations did not differ between men and women, males had significantly higher NK cell activity than age-matched females (20-29 years old). In addition, females on oral contraceptives showed even lower NK cell activity against K562 cells (Yovel et al., 2001).

These studies collectively suggest that using a diverse pool of donors with small experiment numbers presents additional variables that must be noted while interpreting the data.

4.2 Eristostatin and IFN-γ Concentrations

The two M24met runs testify to the points of consideration discussed above. Although both runs showed an upward trend, it was evident that in one experiment, the IFN-γ levels were higher, reaching a maximum of 1468pg/mL at the ten E:T ratio of the control (Figure 8). It can be argued that the NK cells isolated in the first run secreted less IFN-γ than the ones isolated for the second run. If this hypothesis is taken to its logical conclusion, it can be argued that the NK cells isolated in the two runs could have expressed different levels of antigen receptors since the same cell line was used. This can be tested in the future by using labeled antibodies to specific receptors and detecting via flow cytometry.

Recent research reveals that NK cells recognize oligosaccharide structures on the surface of target cells that serve as antigen sites. The sialyl Lewis x oligosaccharides, found on leukemia and epithelial carcinoma cells plays a key role in how effectively NK cells recognize and lyse target cells *in vitro*. Ohyama et. al. showed that sialyl Lewis x oligosaccharide-deficient human melanoma cells were more susceptible to NK lysis *in vitro* when compared to melanoma cells that have the sialyl Lewis x oligosaccharide group (Ohyama et al., 2002). Furthermore, treating the melanoma cells prior to the cytotoxicity assay with anti-sailyl Lewis x antibody inhibited the cytotoxicity of the NK cells (Ohyama et al., 2002). Therefore, it can be deduced that that these structures are essentially antigen sites for melanoma cells. In

addition, aberrant glycosylation of these structures can impair the ability of NK cells to detect and lyse target cells (Benson et al., 2010).

Besides the difference in the two runs, it was evident that in both runs of M24met at the five and ten E:T ratios, the control cells showed higher levels of IFN-γ compared to the eristostatin-treated cells. Due to the low number of experiments, the errors bars suggest that this difference is not notable. To correctly assess statistical significance, the experiment must be repeated more times. At the lower E:T ratios, the eristostatin-treated cells showed higher levels of IFN-γ compared to the control. For the same reasons outlined above, the difference was not notable according to the standard error bars. The assay must be repeated enough times to obtain a P value to assess statistical significance.

Another way to interpret the M24met data is to assume that in one of the runs, an outlier existed. In this case, a trend then becomes more visible. An alternating pattern noted in Figure 9 is evident. The significant of the alternating pattern is discussed below.

With SbCl2 (Figure 6) and MV3 (Figure 5), it was evident that the IFN-γ levels remained below 30pg/mL. However, it must be noted that these experiments were done only once. To make any conclusions about the IFN-γ levels with these two cell lines, more data must be collected. Once again, the alternating pattern is evident, although seemingly reversed for SbCl2 and MV3.

1205Lu, unlike any of the other cell lines, showed a notable difference in IFN-γ levels at the ten E:T ratio. In three runs, an average of 321pg/mL of IFN-γ was detected in the ten E:T ratio of the eristostatin-treated cells compared to just 57pg/mL of IFN-γ in the control, nearly a six-fold increase in IFN-γ levels. In addition, the

eristostatin-treated cells showed a slightly higher IFN-γ at the five E:T ratio, but a lower IFN-γ at the one E:T ratio. The alternating trend is still evident.

With the exception of 1205Lu, no definitive claims can be made about the effect of eristostatin on IFN-γ concentrations without further study. How it is that eristostatin enhanced IFN-γ secretion at the ten E:T ratio is unknown. However, there are hypotheses. Eristostatin may bind NK cells and trigger a pathway that results in the secretion of IFN-γ. This can be ruled out as the sole cause since a similar trend is not evident in all tested cell lines. Another possibility is that eristostatin bound 1205Lu in such a way that made it more apparent to detection by NK cell cells resulting in the production of more IFN-γ. MV3 showed a trend that resembles that of 1205Lu, but requires more data to confirm.

While it may be that eristostatin is making 1205Lu more apparent to detection, it is evident that with SbCl2 and M24met a completely opposite trend is evident. Notably, more data is needed to confirm this. A logical explanation would be that eristostatin is binding and masking antigens on these melanoma cells. It may also be the case that recognition of the antigen on these cells requires a longer contact time which is inhibited by eristostatin.

Another point to address with the IFN-γ data is the apparent alternating trend evident in all cell lines tested (Figure 7). There is no simple explanation for this trend. It is known that NK cells express integrins on their surface including β1, β2, and β3 and freshly insolated NK cells express $\alpha_4\beta_1$, $\alpha_5\beta_1$, $\alpha_1\beta_1$, $\alpha_2\beta_1$, and $\alpha_3\beta_1$ (Rabinowich, 1996). In addition, Interleukin-2 (IL-2) increases the expression of $\alpha_4\beta_1$ and $\alpha_5\beta_1$ (Rabinowich, 1996). Furthermore, it is known that integrins act as signal transducing receptors (Rabinowich, 1996).

It is important to keep in mind that there are numerous activating and deactivating receptors on the surface of NK cells that collectively dictate whether NK cells are activated or not (Vivier et al., 2008). Presumably, it is necessary for NK cells to be in close proximity to melanoma cells to cause lysis. Whether eristostatin actually binds NK cells has never been studied and is simply a matter of speculation. However, lymphocytes in general are known to bind to fibronectin (Sanchez-Aparicio et al., 1994). In addition, activated NK-1 cells (ANK-1) and pre-A-NK, types of precursor NK cell which make up 4-30% of peripheral NK cells, have the ability to interact with fibronectin, laminin, and collagen (Whiteside & Herberman, 1995). Besides these findings, one study in particular suggests that eristostatin binding NK cells is indeed plausible. It was found that lymphocytes, including NK cells, bind fungal hyphal elements via Macrophage-1 (MAC-1) surface structure. Furthermore, it was noted that ligands of MAC-1 including echistatin, a disintegrin, have the ability to inhibit lymphocyte adhesion to *Candida albicans* (Forsyth & Mathews, 2002). This finding acknowledges that echistatin, a disintegrin, does bind NK cells.

Assuming that eristostatin does indeed interact with NK cells, its interaction can be looked at in two ways. It may bind the integrins on the surface of NK cells and brings them closer to activation. It may presumably also occupy the integrin site and not allow the NK cells to attach near their target, in effect inhibiting NK cytotoxicity.

The fact that eristostatin also binds melanoma cell integrins complicates the scenario. Melanoma cells have many integrins which lead to signal transduction. It has been found that jarastatin and flavoridin, two other disintegrins, bind $\alpha_5\beta_1$ which triggers signaling that decreases cell growth of attached B16F10 melanoma cells *in vitro* (Oliva et al., 2007). Oliva acknowledged that binding of other integrins on the cell surface may alter signaling in melanoma cells (Oliva et al., 2007). Therefore,

eristostatin's effect on melanoma cells depends on the set of integrins on their surface and what signaling cascade they trigger.

Overall, when putting all of these interactions together, the system is indeed highly complex and differs for each cell line. For 1205Lu, it may be that eristostatin binds on the surface and in one way or another leads 1205Lu to become more apparent to NK cells which release more cytokines. This is mere speculation and must be tested to confirm or deny. For the cells showing an alternating pattern (Figure 7), a dual mechanism may exist. Eristostatin may be interacting with NK cells in a certain way while also reacting with melanoma cells in another way. However, basic consideration must also be noted. Many of these experiments were performed only once.

4.3 Eristostatin and TNF-α Concentrations

Just like IFN-γ levels, 1205Lu (Figure 14) showed higher TNF-α levels at the zero, five, and ten E:T ratios. The one E:T ratio showed the opposite result, such that the control had higher levels of TNF-α. The experiment was done only once. Therefore, error bars are not applicable. In addition, TNF-α levels never went above 50pg/mL and the difference between the control and the eristostatin-treated 1205Lu cells was not very great. However, the difference coincides with the IFN-γ data discussed for 1205Lu.

SbCl2 (Figure 11) showed a pattern that is similar to that discussed for 1205Lu. However, the pattern did not match that of IFN-γ for SbCl2. Furthermore, the levels of TNF-α were even lower than 1205Lu, reaching a maximum at 26pg/mL. MV3 showed an upward trend. The eristostatin-treated cells showed higher levels of TNF-α at the zero, one, and five E:T ratios, and a lower T:E ratio at the ten E:T ratio. M24met also followed the trend of MV3 where the eristostatin-treated cells showed a

higher TNF-α at the zero, one, and five E:T ratios and a lower TNF-α concentration at the ten E:T ratio. MV3 and M24met TNF-α notably did not follow the pattern suggested by the IFN-γ data. Like IFN-γ, similarities between the cell lines are evident. As discussed above, the mechanism is highly complex. It seems that the alternating function (Figure 7) is no longer present with MV3 and M24met. The ratios through five E:T follow a trend and switch at ten. However, it is still apparent for 1205Lu and SbCl2.

4.4 Cytotoxicity Overview

There are two ways to look at the cytotoxicity data, both of which provide valuable insight into the interaction of melanoma cells, NK cells, and eristostatin. One way to evaluate the data is to look at the background percent lysis (just melanoma cells). Another way is to subtract the initial luminescence for CytoTox-Glo or lysis percentage for flow cytometry of the eristostatin-treated cells from all the eristostatin-treated ratios and to subtract the initial luminescence or percent lysis of the control from all the control ratios as described above.

It is also important to note that the flow cytometry data represents a cytotoxicity of NK incubated with melanoma cells for three hours while the CytoTox-Glo represents cytotoxicity of NK incubated with melanoma cells overnight. The cytokine data also represents an overnight incubation.

For 1205Lu (Figure 20), from the raw data it appears that the control is more sensitive to NK lysis. There is a notable difference between the control and the eristostatin-treated cells at the zero (background) and 0.5 E:T ratio. The zero E:T ratio is a well that has only 1205Lu cells in it. The fact that the control percent lysis is notably higher than the eristostatin-treated 1205Lu percent lysis suggests that eristostatin enhances the survival of 1205Lu *in vitro* for the first three hours of

incubation (Figure 26). Why it is that eristostatin enhances the survivability of 1205Lu *in vitro* remains to be investigated. It could be that eristostatin binds integrins and triggers secondary messenger pathways that "tell" the cell it is in a favorable environment for growth and proliferation or may trigger secondary messengers that short circuit some apoptosis mechanisms.

In spite of this finding, it is important to see if the NK lytic ability is enhanced by eristostatin. In order to do this, the initial lysis was subtracted as described above. This essentially sets the initial lysis to zero in order to interpret the other ratios. This analysis reveals that the control on average still shows a higher percent lysis. The difference, however, is not notable according to the standard error bars. If the experiments were repeated enough times, and the difference was found to be statistically significant, the data would suggest that eristostatin was inhibiting the lytic ability of NK cells. This could be done by masking melanoma cell antigens that would otherwise trigger NK lysis. It could also shorten the interaction time by not allowing NK cell integrins to bind the matrix around melanoma cells.

The CytoTox-Glo data for 1205Lu (Figure 15) portrays a different pattern. Once again, the difference in the length of incubation must be noted. After an overnight incubation, it appeared that eristostatin inhibited the survivability of 1205Lu compared to the control (Figure 19). This suggests a dual mechanism where eristostatin initially enhanced survivability of 1205Lu and later began to inhibit it. The mechanics of this trend have yet to be investigated and are worthy of further research. Unlike the flow cytometry data, the CytoTox-Glo data suggested that eristostatin-treated cells on average showed a much closer percent lysis compared to the control. At the ten E:T ratio, the eristostatin-treated cells show a higher percent lysis than the control. The difference, however, was not significant according to the standard error bars.

The C8161 (Figure 21) flow cytometry raw data suggested a similar trend to 1205Lu such that the control showed a higher percent lysis when compared to the eristostatin-treated cells. Remarkably, the difference was notable according to the standard error bars at all ratios except at the 2.5 and three E:T ratios. Once again, the zero E:T ratio suggested that C8161 survivability was enhanced by eristostatin.

When the initial lysis was subtracted as noted above, the percent lysis difference was much closer. However, it is notable that at the ten E:T ratio, the control maintained a higher percent lysis compared to the eristostatin-treated cells. This suggested that eristostatin did slightly inhibit the ability to NK cells to lyse C8161 at the ten E:T ratio. This may be due to the masking concept referred to above. Further studies are required to test this hypothesis.

With CytoTox-Glo, the initial lysis suggested no notable difference existed between the control and the eristostatin-treated C8161 cells although the control showed a 3% higher percent lysis. The control showed higher percent lysis on average throughout the run with all ratios. However, the difference was not notable according to the standard error bars except at the one E:T ratio.

Like C8161 and 1205Lu, M24met raw flow data suggested that eristostatin enhanced the survivability of M24met after a three hour incubation compared to the control. However, at the 0.5 and 2.5 E:T ratio, the eristostatin-treated cells showed a higher percent lysis than the control. Once the initial lysis is subtracted, the trend was more obvious. Although the percent lysis was relatively low across the ratios, eristostatin at lower E:T ratios seemed to be enhancing the lytic ablity of NK cells. However, it must be noted that this experiment was done only once and more data is needed to verify this trend.

The CytoTox-Glo data for M24met showed the initial lysis was slightly higher for the control than the eristostatin-treated cells. Since the experiment was done once, this suggestion should be taken with appropriate caution. For the rest of the ratios, the difference between the eristostatin-treated cells and the control seem to be minimal where at the one and five E:T ratio, the control shows a higher percent lysis and at the ten E:T ratio, the eristostatin-treated cells show a higher percent lysis.

The flow cytometry data for WM164 also seemed to follow a trend presented by M24met such that the eristostatin-treated cells exceeded the control at the 0.5 E:T ratio. At all other ratios including the zero E:T ratio, the control showed a higher percent lysis. Excluding the 0.5 E:T ratio, the differences with WM164 were not significant according to the standard error bars. However, once the initial lysis was subtracted to account for the increased survivability of WM164 with eristostatin, it was apparent that eristostatin does enhance the lytic ability of NK cells toward WM164 at the 0.5 E:T ratio. This difference was notably significant according to the standard error bars. At the higher ratios, the control seemed to present with a higher percent lysis than the eristostatin-treated cells.

CytoTox-Glo data for WM164 showed that the initial lysis of the eristostatin-treated cell is minutely higher than the control. It was also higher at the one E:T ratio. However, the control showed a higher percent lyis at the five and ten E:T ratio. Statistical significance did not apply since the experiment was done once. However, CytoTox-Glo data agreed with the flow data except at the zero E:T ratio.

MV3 also appeared to survive at higher rates when incubated with eristostatin. The control presented with higher percent lysis at all ratios except at the 2.5 E:T ratio. Once the initial lysis was subtracted, this difference became more obvious as eristostatin seems to be enhancing the lytic ability of NK cells toward MV3 cells. The

difference, however, is not significant according to the standard error bars. No CytoTox-Glo data was collected for this cell line.

SbCl2 showed a pattern that differed from all other cell lines. At the zero E:T zero ratio, the eristostatin-treated cells showed a slightly higher percent lysis than the control, although the difference was not significant according to the standard error bars. However, once the initial lysis was subtracted, it was evident that eristostatin enhanced the lytic ability of NK toward SbCl2 which was obvious at the 2.5 E:T ratio were the difference was significant according to the standard error bars. The difference decreased at the three E:T ratio and is no longer significant according to the standard error bars. No CytoTox-Glo data was collected for this cell line.

4.5 Cytotoxicity

As discussed above, this study is highly complex and care must be taken when evaluating the data. To attest to this complexity, it has been shown that if washed after treatment, eristostatin-treated SbCl2 cells with untreated TALL-104 cells yielded a higher percent lysis than if TALL-104 cells and SbCl2 cells were both treated with eristostatin (McLane et al., 2001). However, there are some patterns that can be interpreted. Several general main points can be acquired from this study.

It is apparent that after a three hour incubation, eristostatin enhanced the survivability of 1205Lu, C8161, M24met, and to a lesser extend MV3. It seemed to have little impact on SbCl2 survivability after a three hour incubation. It must be noted that SbCl2 is the only radial growth phase melanoma cell used in this study. As discussed earlier, there are different integrins on each melanoma cell line. What type of secondary signaling cascade they trigger is unknown. How eristostatin enhanced the survivability of certain melanoma cell is a novel question worthy of further research.

After a 24 hour incubation, the CytoTox-Glo assay suggested that eristostatin had very little impact on the survivability of C8161, M24met, and WM164. MV3 was not tested with CytoTox-Glo. This suggested that the enhancement of survivability at three hours is no longer evident for these cell lines. However, it appears that eristostatin inhibited the survivability of 1205Lu at 24 hours. The mechanism is still unclear. However, cells that incubated overnight have time to multiply, introducing another factor into the study. This novel finding with 1205Lu encourages further studies.

To judge the effect of eristostatin on the ability of NK cells to lyse melanoma cells, it is important to bypass the discrepancy in melanoma cell survivability. The adjusted curves were designed to overcome this obstacle. In every well, the total number of melanoma cells was constant. Therefore, the modified data theoretically represents the true effect of eristostatin on NK cell lysis of melanoma cells.

From the 24 hour incubation using CytoTox-Glo, concrete conclusions can not be made concerning eristostatin's affect on NK cells' ability to lyse 1205Lu or M24met since the difference in percent lysis is minimal. It is apparent that eristostatin, however, impacted the ability of NK cells to lyse other melanoma cells at select ratios. Eristostatin inhibited the cytotoxicity of NK cells toward C8161 melanoma cells at the 0.5 E:T ratio. Eristostatin also presumably inhibits NK cytotoxicity toward WM164. More data is needed to confirm this.

Using the three hour incubation data, no definitive conclusions about the effects of NK cytotoxicty toward 1205Lu and MV3 can be made. However, it is apparent that eristostatin suppressed the lytic ability of NK cells toward C8161 at the ten E:T ratio. However, eristostatin did enhance the lytic ability of NK cells toward

M24met at E:T ratios below five, SbCl2 at the 2.5 E:T ratio, and WM164 at the 0.5 E:T ratio after a three hour incubation.

The complexity of the interactions and the fact that eristostatin interacts with both melanoma cells and NK cells simply does not lead to a simple all encompassing answer to "does eristostatin enhance the lytic ability of NK cells toward melanoma cells?" In terms of eristostatin as a possible therapeutic for select melanoma cells at select phases, the complexity of this study does not permit a simple answer.

4.6 Three Dimensional Studies

The finding of the three dimensional data were non-remarkable for differences between eristostatin and the control for C8161. No spatial configuration differences, differences in live/dead ratios, or in formed structures were observed between the eristostatin-treated cells and the control.

It must be noted that this finding is not surprising considering the makeup of the Matrigel®. Matrigel® is comprised primarily of laminin, followed by collagen IV, heparin sulfate proteoglycans, and entactin/nidogen. Matrigel® also contains growth factors. To begin our three-dimensional studies, we carried out a live/dead assay in Matrigel® to see if cells incubated with eristostatin in a 3D environment exhibited similar live/dead ratios compared to cells incubated without eristostatin. It was found that cells in Matrigel® with eristostatin and without eristostatin did not exhibit a difference. It should be noted that eristostatin does not have inhibitory activity against cell adhesion to laminin or collagen (McLane et al., 2008). Since eristostatin inhibited melanoma cell migration on fibronectin (FN), future experiments will incorporate FN into the matrix (McLane et al., 2008).

REFERENCES

Anfossi, N., Andre, P., Guia, S., Falk, C. S., Roetynck, S., Stewart, C. A., Breso, V., Frassati, C., Reviron, D., Middleton, D., Romagne, F., Ugolini, S., & Vivier, E. (2006). Human NK cell education by inhibitory receptors for MHC class I. *Immunity, 25*(2), 331-342. doi:10.1016/j.immuni.2006.06.013

Benson, V., Grobarova, V., Richter, J., & Fiserova, A. (2010). Glycosylation regulates NK cell-mediated effector function through PI3K pathway. *International Immunology, 22*(3), 167-177. doi:10.1093/intimm/dxp123

Bregman, M. D., Funk, C., & Fukushima, M. (1986). Inhibition of human melanoma growth by prostaglandin A, D, and J analogues. *Cancer Research, 46*(6), 2740-2744.

Clark, W. H. (1991). Tumour progression and the nature of cancer. *British Journal of Cancer, 64*(4), 631-644.

Cooper, M. A., Fehniger, T. A., & Caligiuri, M. A. (2001). The biology of human natural killer-cell subsets. *Trends in Immunology, 22*(11), 633-640.

Danen, E. H., Marcinkiewicz, C., Cornelissen, I. M., van Kraats, A. A., Pachter, J. A., Ruiter, D. J., Niewiarowski, S., & van Muijen, G. N. (1998). The disintegrin eristostatin interferes with integrin alpha 4 beta 1 function and with experimental metastasis of human melanoma cells. *Experimental Cell Research, 238*(1), 188-196. doi:10.1006/excr.1997.3821

Facchini, A., Mariani, E., Mariani, A. R., Papa, S., Vitale, M., & Manzoli, F. A. (1987). Increased number of circulating leu 11+ (CD 16) large granular lymphocytes and decreased NK activity during human ageing. *Clinical and Experimental Immunology, 68*(2), 340-347.

Forsyth, C. B., & Mathews, H. L. (2002). Lymphocyte adhesion to candida albicans. *Infection and Immunity, 70*(2), 517-527.

Furusawa, K., Tajima, F., Tanaka, Y., Ide, M., & Ogata, H. (1998). Short-term attenuation of natural killer cell cytotoxic activity in wheelchair marathoners with paraplegia. *Archives of Physical Medicine and Rehabilitation, 79*(9), 1116-1121.

Helson, L., Green, S., Carswell, E., & Old, L. J. (1975). Effect of tumour necrosis factor on cultured human melanoma cells. *Nature, 258*(5537), 731-732.

Herlyn, D., Iliopoulos, D., Jensen, P. J., Parmiter, A., Baird, J., Hotta, H., Adachi, K., Ross, A. H., Jambrosic, J., & Koprowski, H. (1990). In vitro properties of human melanoma cells metastatic in nude mice. *Cancer Research, 50*(8), 2296-2302.

Humphries, M. J., Travis, M. A., Clark, K., & Mould, A. P. (2004). Mechanisms of integration of cells and extracellular matrices by integrins. *Biochemical Society Transactions, 32*(Pt 5), 822-825. doi:10.1042/BST0320822

Juhasz, I., Albelda, S. M., Elder, D. E., Murphy, G. F., Adachi, K., Herlyn, D., Valyi-Nagy, I. T., & Herlyn, M. (1993). Growth and invasion of human melanomas in human skin grafted to immunodeficient mice. *The American Journal of Pathology, 143*(2), 528-537.

McLane, M. A., Joerger, T., & Mahmoud, A. (2008). Disintegrins in health and disease. *Frontiers in Bioscience : A Journal and Virtual Library, 13*, 6617-6637.

McLane, M. A., Kowalska, M. A., Silver, L., Shattil, S. J., & Niewiarowski, S. (1994). Interaction of disintegrins with the alpha IIb beta 3 receptor on resting and activated human platelets. *The Biochemical Journal, 301 (Pt 2)*(Pt 2), 429-436.

McLane, M. A., Kuchar, M. A., Brando, C., Santoli, D., Paquette-Straub, C. A., & Miele, M. E. (2001). New insights on disintegrin-receptor interactions: Eristostatin and melanoma cells. *Haemostasis, 31*(3-6), 177-182.

McLane, M. A., Zhang, X., Tian, J., Zelinskas, C., Srivastava, A., Hensley, B., & Paquette-Straub, C. (2005). Scratching below the surface: Wound healing and alanine mutagenesis provide unique insights into interactions between eristostatin, platelets and melanoma cells. *Pathophysiology of Haemostasis and Thrombosis, 34*(4-5), 164-168. doi:10.1159/000092417

Moretta, L., & Moretta, A. (2004). Unravelling natural killer cell function: Triggering and inhibitory human NK receptors. *The EMBO Journal, 23*(2), 255-259. doi:10.1038/sj.emboj.7600019

Mueller, B. M., Romerdahl, C. A., Trent, J. M., & Reisfeld, R. A. (1991). Suppression of spontaneous melanoma metastasis in scid mice with an antibody to the epidermal growth factor receptor. *Cancer Research, 51*(8), 2193-2198.

Murray, J., Barbara, J. A., Dunkley, S. A., Lopez, A. F., Van Ostade, X., Condliffe, A. M., Dransfield, I., Haslett, C., & Chilvers, E. R. (1997). Regulation of neutrophil apoptosis by tumor necrosis factor-alpha: Requirement for TNFR55 and TNFR75 for induction of apoptosis in vitro. *Blood, 90*(7), 2772-2783.

Ohyama, C., Kanto, S., Kato, K., Nakano, O., Arai, Y., Kato, T., Chen, S., Fukuda, M. N., & Fukuda, M. (2002). Natural killer cells attack tumor cells expressing high levels of sialyl lewis x oligosaccharides. *Proceedings of the National Academy of Sciences of the United States of America, 99*(21), 13789-13794. doi:10.1073/pnas.212456599

Oliva, I. B., Coelho, R. M., Barcellos, G. G., Saldanha-Gama, R., Wermelinger, L. S., Marcinkiewicz, C., Benedeta Zingali, R., & Barja-Fidalgo, C. (2007). Effect of RGD-disintegrins on melanoma cell growth and metastasis: Involvement of the actin cytoskeleton, FAK and c-fos. *Toxicon : Official Journal of the International Society on Toxinology, 50*(8), 1053-1063. doi:10.1016/j.toxicon.2007.07.016

Rabinowich, H. (1996). Integrins as signal transducing receptors on NK cells. *Methods (San Diego, Calif.), 9*(2), 362-369.

Reintgen, C., Shivers, S., Reintgen, M., Giuliano, R., & Reintgen, D. (2010). The changing face of malignant melanoma. *Journal of Surgical Oncology, 101*(6), 443-446. doi:10.1002/jso.21515

Sanchez-Aparicio, P., Dominguez-Jimenez, C., & Garcia-Pardo, A. (1994). Activation of the alpha 4 beta 1 integrin through the beta 1 subunit induces recognition of the RGDS sequence in fibronectin. *The Journal of Cell Biology, 126*(1), 271-279.

Schroder, K., Hertzog, P. J., Ravasi, T., & Hume, D. A. (2004). Interferon-gamma: An overview of signals, mechanisms and functions. *Journal of Leukocyte Biology, 75*(2), 163-189. doi:10.1189/jlb.0603252

Sturm, R. A., Satyamoorthy, K., Meier, F., Gardiner, B. B., Smit, D. J., Vaidya, B., & Herlyn, M. (2002). Osteonectin/SPARC induction by ectopic beta(3) integrin in human radial growth phase primary melanoma cells. *Cancer Research, 62*(1), 226-232.

Urso, C. (2004). Are growth phases exclusive to cutaneous melanoma? *Journal of Clinical Pathology, 57*(5), 560.

van der Flier, A., & Sonnenberg, A. (2001). Function and interactions of integrins. *Cell and Tissue Research, 305*(3), 285-298.

van Muijen, G. N., Jansen, K. F., Cornelissen, I. M., Smeets, D. F., Beck, J. L., & Ruiter, D. J. (1991). Establishment and characterization of a human melanoma cell line (MV3) which is highly metastatic in nude mice. *International Journal of Cancer.Journal International Du Cancer, 48*(1), 85-91.

Vassalli, P. (1992). The pathophysiology of tumor necrosis factors. *Annual Review of Immunology, 10*, 411-452. doi:10.1146/annurev.iy.10.040192.002211

Vivier, E., Tomasello, E., Baratin, M., Walzer, T., & Ugolini, S. (2008). Functions of natural killer cells. *Nature Immunology, 9*(5), 503-510. doi:10.1038/ni1582

Whiteside, T. L., & Herberman, R. B. (1995). The role of natural killer cells in immune surveillance of cancer. *Current Opinion in Immunology, 7*(5), 704-710.

Wierzbicka-Patynowski, I., Niewiarowski, S., Marcinkiewicz, C., Calvete, J. J., Marcinkiewicz, M. M., & McLane, M. A. (1999). Structural requirements of echistatin for the recognition of alpha(v)beta(3) and alpha(5)beta(1) integrins. *The Journal of Biological Chemistry, 274*(53), 37809-37814.

Yovel, G., Shakhar, K., & Ben-Eliyahu, S. (2001). The effects of sex, menstrual cycle, and oral contraceptives on the number and activity of natural killer cells. *Gynecologic Oncology, 81*(2), 254-262. doi:10.1006/gyno.2001.6153